UNIVERSITY OF MINNESOTA
ST. ANTHONY FALLS HYDRAULIC LABORATORY

Project Report No. 112

Friction Factors For Helical Corrugated Aluminum Pipe

by
EDWARD SILBERMAN
and
WARREN Q. DAHLIN

Prepared for
THE ALUMINUM ASSOCIATION
New York, New York

DECEMBER 1969

MINNEAPOLIS, MINNESOTA

CONTENTS

LIST OF ILLUSTRATIONS

LIST OF TABLES

LIST OF SYMBOLS

A = area, ft^2

D = inside diameter of test pipe, ft

f = Darcy friction factor

g = acceleration due to gravity, ft/sec^2

h = head loss in pipe, ft

L = length of pipe, ft

n = Manning roughness coefficient

P = perimeter, ft

Q = discharge, cfs

R_h = hydraulic radius = A/P, ft

R = radius, ft

Re = Reynolds number = $\overline{V}D/\nu$

S = slope of hydraulic grade line = h/L

U = local velocity component parallel to axis of pipe = V Cos α, fps

U_{max} = maximum local velocity component parallel to axis of pipe, fps

V = magnitude of local velocity, fps

$\overline{V}$ = average axial velocity = Q/A, fps

V_* = shear velocity = $\sqrt{\tau_o/\rho}$ = $\overline{V}\sqrt{f/8}$, fps

Y = vertical distance from pipe invert to hydraulic grade line at exit, ft

y = vertical distance from wall of pipe, ft

α = angle between velocity vector and axis of pipe, deg

θ = helix angle of corrugation measured from axial direction, deg

ε = kinematic eddy viscosity, ft^2/sec

ν = kinematic viscosity, ft^2/sec

ρ = density, lb sec^2/ft^4

τ_o = shear stress, lb/ft^2

FRICTION FACTORS FOR HELICAL CORRUGATED ALUMINUM PIPE

I. INTRODUCTION

The St. Anthony Falls Hydraulic Laboratory was engaged by the Aluminum Association to determine the friction factors for fully developed flow in helical corrugated pipe of several sizes. The pipe was furnished by Kaiser Aluminum and Chemical Sales, Inc., in 24 in., 18 in., and 12 in. nominal diameters. Pipe characteristics are shown in Fig. 1.

One hundred feet of each size of pipe were supplied in two 40 ft lengths and one 20 ft length. Field bonding materials were provided for joints, while flanges were supplied for connecting the 20 ft length of each size pipe to the laboratory water supply and one of the 40 ft lengths to the discharge control valve. Helical seams used in fabricating the pipe were sealed with sealing compound at the factory according to a standard method, and these seams did not leak during the experiments.

II. EXPERIMENTAL METHOD

The pipe was installed in the laboratory flow system as indicated in Fig. 2 and shown in Fig. 3. Water passed through a shut-off valve and three right-angled guide vane bends before entering the test pipe. The first 20 ft length of test pipe and a good deal of the next 40 ft served as entry length to produce fully developed flow. The exact length required for entry varied with pipe diameter and is shown later in the hydraulic grade line diagrams. Another control valve was placed at the downstream end of the pipeline.

The test pipe discharged into a channel from which the flow could be directed into either the laboratory weighing tanks (up to 15 cfs) or the laboratory volumetric tanks (up to 300 cfs). These tanks are calibrated and produce measurements which are accurate within about 0.1 per cent for the weighing tanks and about 0.5 per cent for the volumetric tanks. The pipe was laid on wood sleepers placed every 5 ft at a grade of 0.002 ft/ft measured after it was filled with water by closing the downstream valve. The pipe was relatively free to expand laterally, side bracing blocks

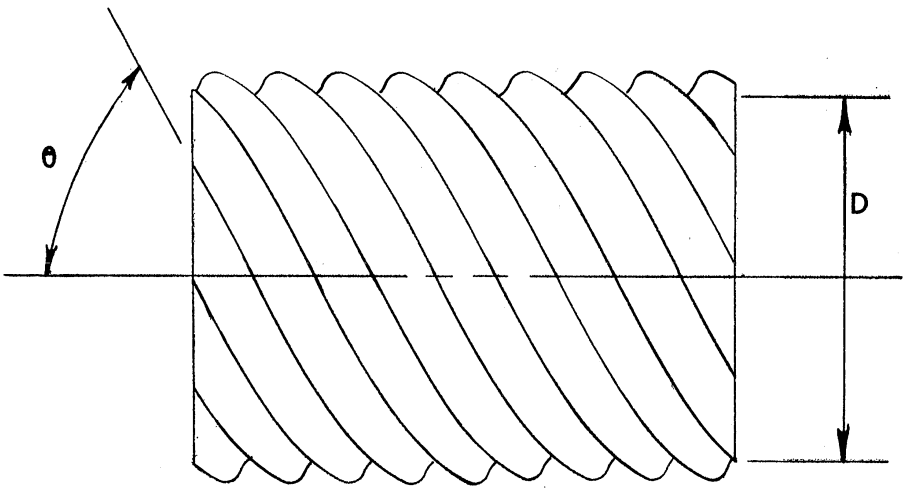

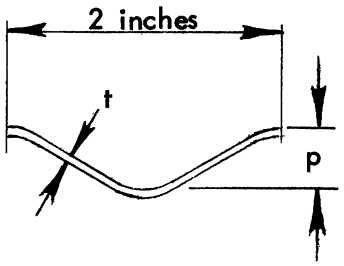

Form of Corrugation

Nominal Pipe Dia. in.	Average Measured Dia. D-in.	Helix Angle θ - Deg *	t - in. *	p - in. *
24	23.974	75	0.075	0.500
18	18.098	70	0.060	0.438
12	11.9127	59-1/2	0.060	0.438

*From factory specifications

Fig. 1 - Pipe Details

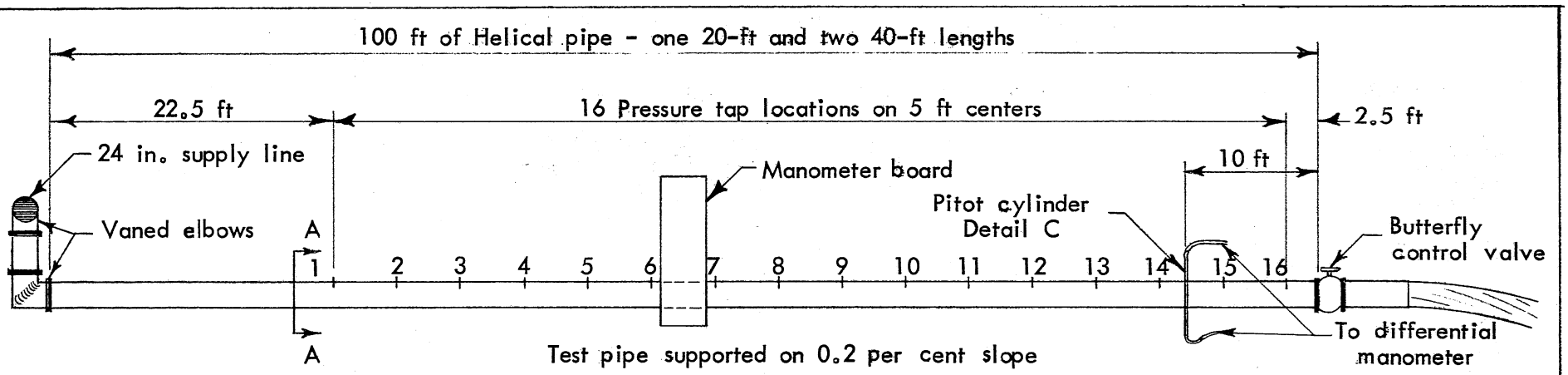

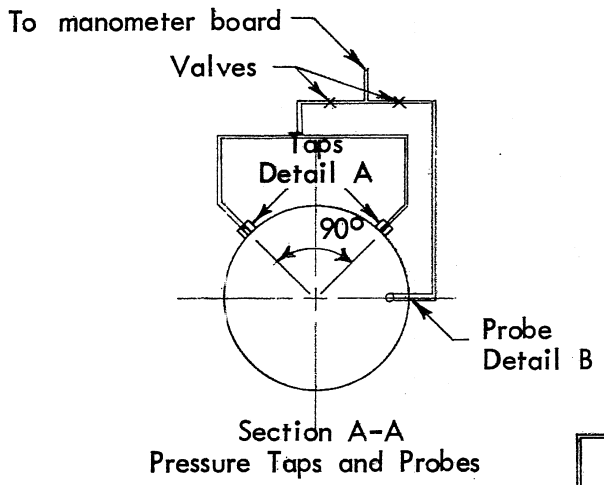

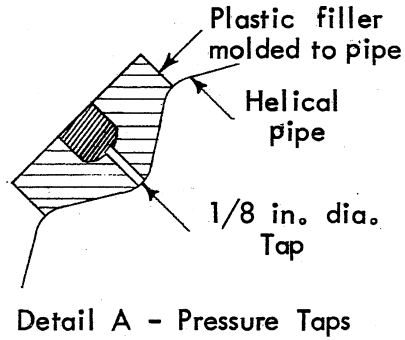

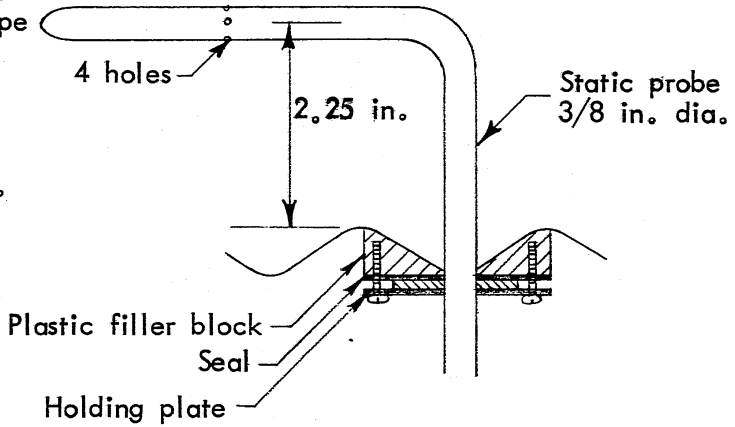

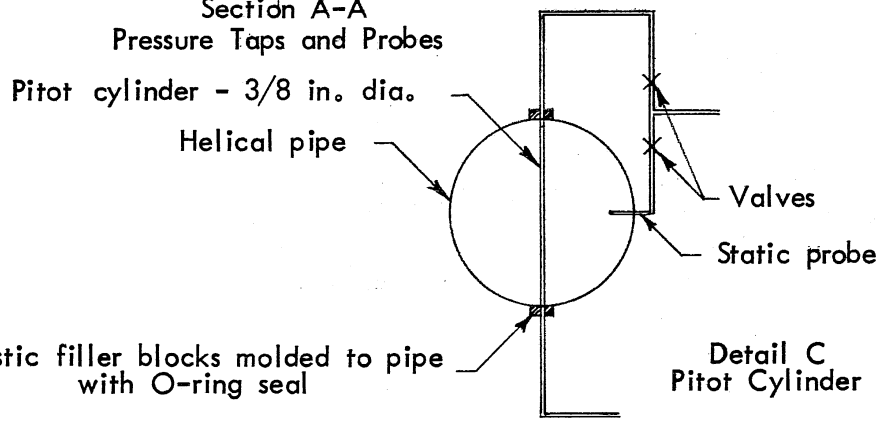

Fig. 2 - Test Arrangement

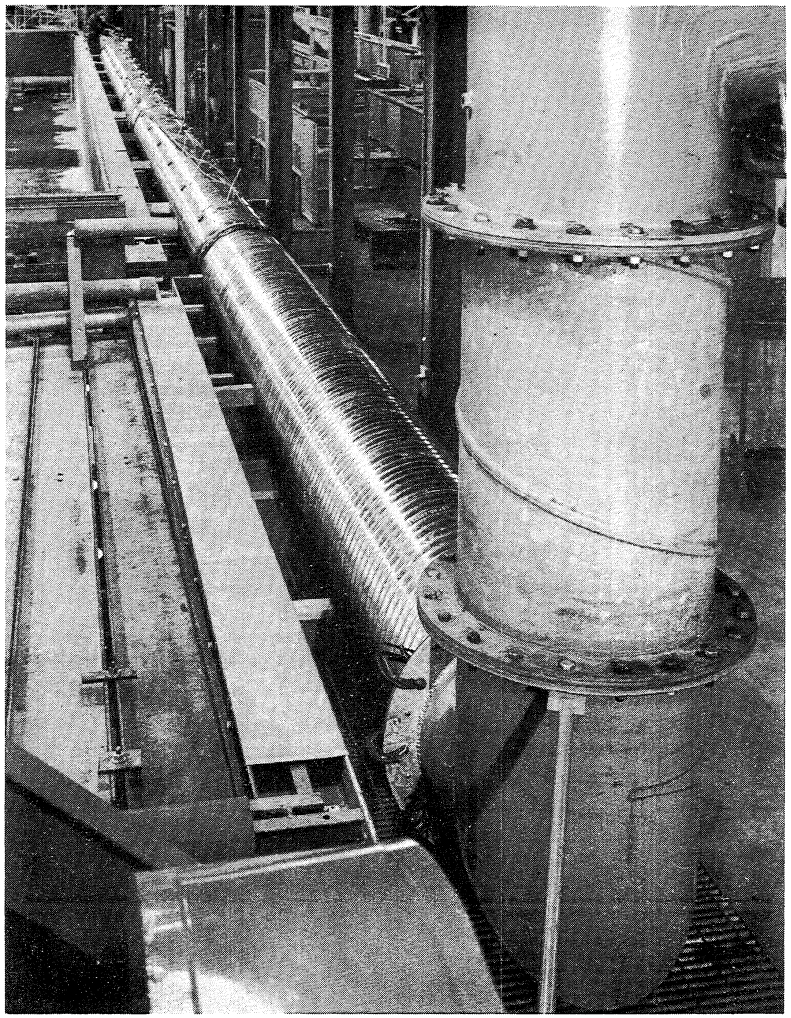

a. Looking Downstream, 24 in. Pipe Installed

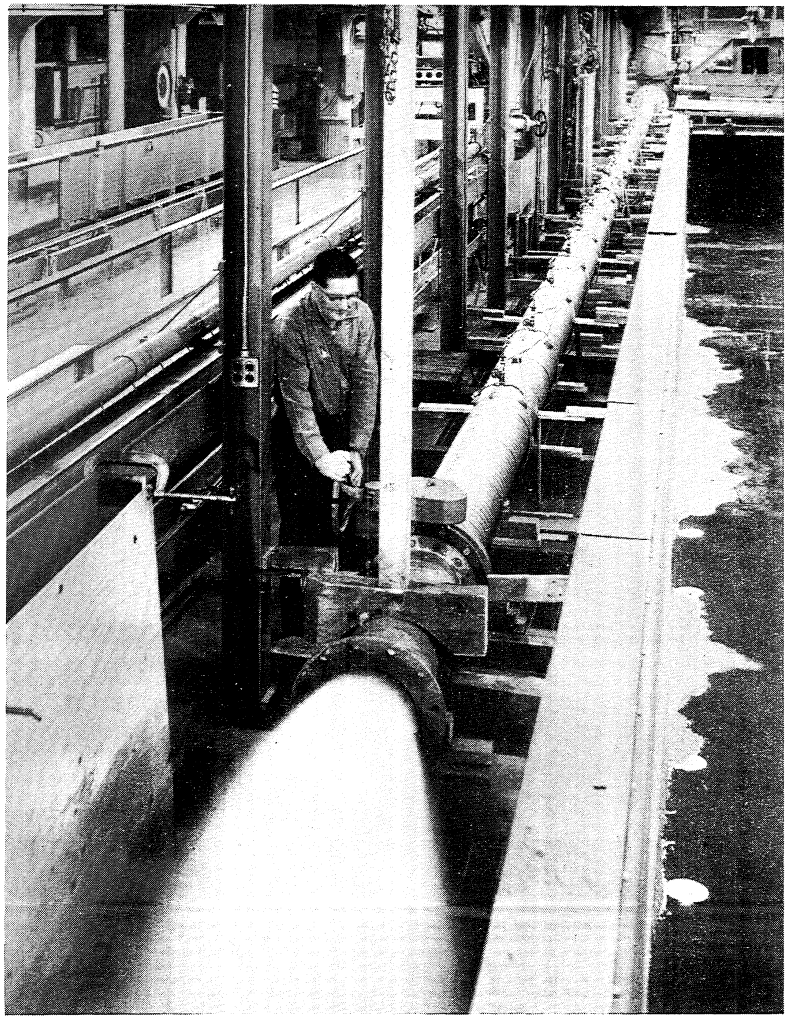

b. Looking Upstream, 12 in. Pipe Installed

Fig. 3 - Two Views of the Experimental Arrangement

being placed about every 10 ft, and measurements showed that it was slightly out of round when filled with water.

During the laying of the pipe care was taken to match the corrugations at the joints and to prevent the intrusion of joint-sealing material from the thermofit heat-shrinkable couplers used at the joints. The sealer was a thermoplastic sealant or asphalt-like material with a polyolefin sheet backing which was applied with heat. A metal collar was placed over this to insure against any leakage, as shown in Fig. 4. Sealer intrusion was prevented by taping the joint with cloth or fiber tape before application of the coupler material. This care was taken to assure that there would not be inordinate joint losses. Inspection of the pipe, which involved both measurement from the outside and visual observations from inside by a man who crawled inside the larger pipes, showed that the pipe was straight and closely uniform throughout its length.

Before installation the downstream 40 ft length of pipe and part of the middle 40 ft length were provided with a system of piezometer taps. These consisted of flush-mounted wall taps interconnected in pairs every 5 ft along the pipe as shown in detail in Fig. 2 and in Fig. 5. The taps were placed at the bottoms of the corrugations (points of smallest diameter) even though it was known from the work of Webster and Metcalf [1]* that more error in location could be tolerated if the taps were at the tops of the corrugations. The method of locating the taps by first drilling a hole through the pipe wall, then inserting a wire in the hole, and finally casting a plastic material around the wire to hold the body of the piezometer connector proved to be very accurate in locating the hole and was most accurately done by placing the holes at the bottoms of the corrugations. Piezometer tap positions were sometimes shifted a fraction of an inch from exact 5 ft spacing so that they could be placed at the exact bottoms of the corrugations. The piezometers connected to a central manometer board.

On the 24 in. pipe only, a second piezometer system was installed. This consisted of Pitot static tubes inserted 2-1/4 inches into the

*Numbers in brackets refer to the list of references on page 41.

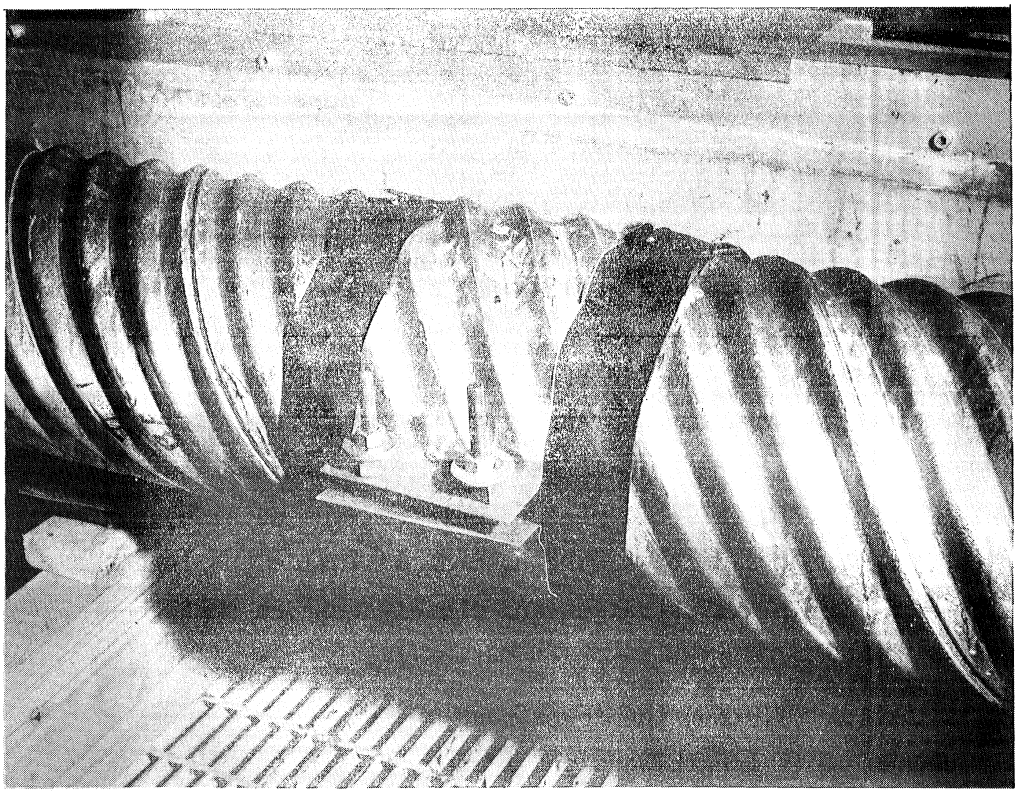

Fig. 4 - A Typical Joint in the Pipes

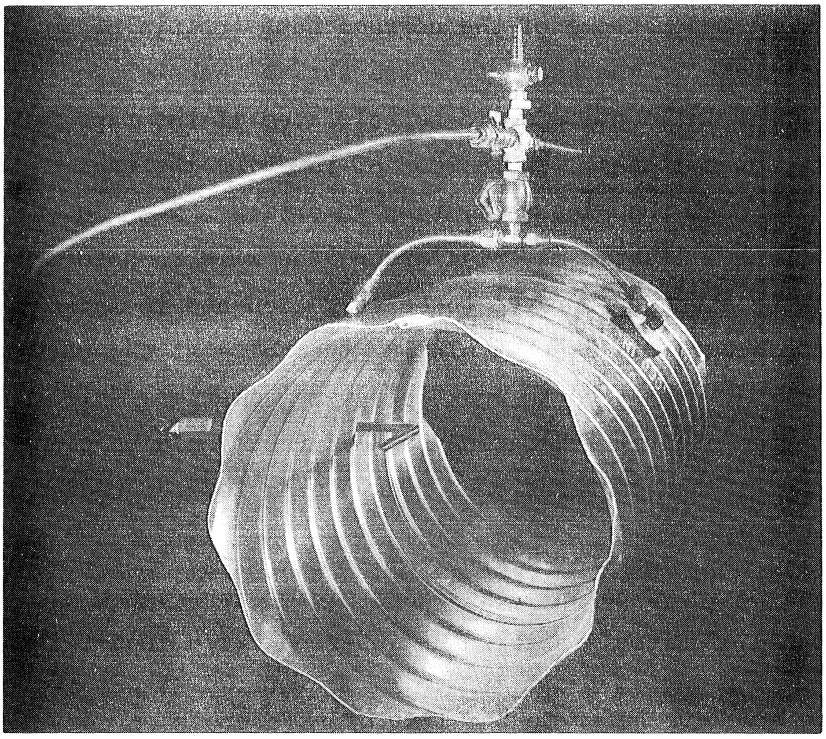

Fig. 5 - The Piezometer Tap Systems

pipe along a horizontal diameter at 5 ft intervals; details are shown in Figs. 2 and 5. The purpose of the dual piezometer system was to assure that the pressure drop was the same in the interior of the pipe as on the walls. This check was necessary because of the spiral flow in the pipe. The circumferential component of the spiral flow produces a radial pressure gradient with higher pressures on the wall and lower pressures on the axis. If the circumferential component of the flow is not fully developed, the measured pressure drop on the wall will be less than that in the interior due to the developing radial pressure gradient.

Hence, a preliminary set of runs was made in the 24 in. pipe (in the manner described later) at 12 discharges between maximum and minimum. At each discharge, pressures were measured at the manometer board for each pair of wall taps and for each static probe without changing the flow conditions. The slopes of the grade lines were compared and were found to be practically identical, especially for the last 20 or 25 ft. Even for longer distances the slopes did not vary by more than 0.3 of one per cent (the slope being greater for the static probes). It was therefore concluded that the flow was fully developed, including the rotational component.

Since some effort was involved in installing the static probes and considerable time consumed in aligning them with the flow, and since there appeared to be a very slight increase in head loss with the probes installed, it was decided to omit the static probes in the 18 in. and 12 in. pipe tests. The tests on the 24 in. pipe, too, were later rerun without the static probes, and it is these data which are reported subsequently.

Ten feet from the downstream end of each pipeline, as shown in Fig. 2, a pair of glands was provided, one at each end of a vertical diameter, for inserting a Pitot cylinder to measure velocity magnitude and direction. The glands provided for a 3/8-inch-diameter cylinder. Adjacent to this location and 90 deg from the Pitot cylinder glands a special gland was provided for insertion of one of the Pitot static tubes along a horizontal diameter to permit obtaining static pressure for use with the total heads from the Pitot cylinder.

A test run consisted of establishing a given discharge through the pipeline by regulating the downstream valve, measuring the discharge and the water temperature, reading the manometer elevations from each tap position on the central manometer board (Fig. 6), and checking the discharge again. Manometers fluctuated considerably in some of the runs, and the readings were obtained as visual averages. It took from 30 to 45 minutes to complete one run. A number of runs were made for each pipe size, beginning with the largest discharge possible for that size, to develop the friction-factor-versus-Reynolds-number curve. Final runs were made with the downstream valve removed to obtain maximum Reynolds numbers.

In addition one special run was made for each pipe size in which velocity profiles along a vertical diameter were measured along with discharge and water temperature.

III. DETERMINATION OF FRICTION FACTOR

The Darcy friction factor f and the Manning roughness coefficient n were computed from the test data for each run and plotted against Reynolds number Re. The Darcy friction factor f is defined by the equation

$$h = f \frac{L}{D} \frac{\bar{V}^2}{2g} \qquad (1)$$

With S equal to h/L, f equals $\frac{2gDS}{\bar{V}^2}$. This formula was used in computing f.

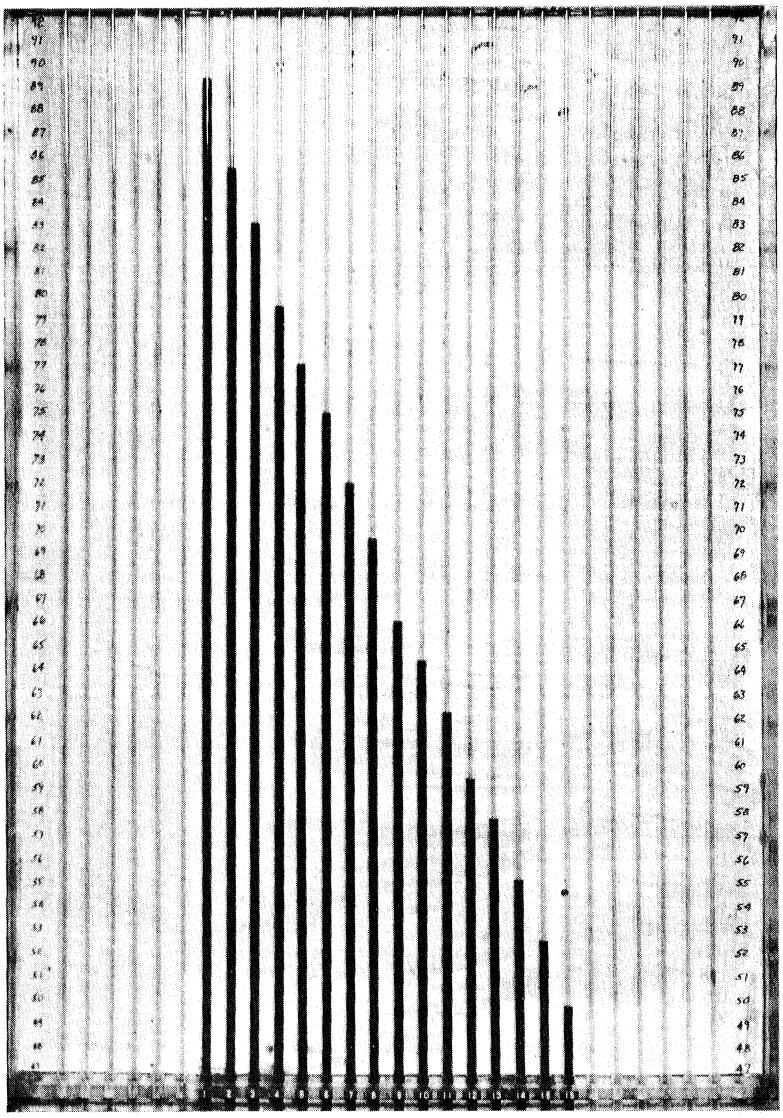

Fig. 6 - The Manometer Board with a Discharge of approximately 35 cfs through the 24 in. pipe

The Manning roughness coefficient n is defined by the equation

$$\overline{V} = \frac{1.486}{n} R_h^{2/3} S^{1/2} \quad \text{or} \quad n = \frac{1.486\, R_h^{2/3} S^{1/2}}{\overline{V}} \tag{2}$$

from which n was computed. This equation is in the English system of units.

The Reynolds number was computed from

$$\text{Re} = \frac{\overline{V}D}{\nu} \tag{3}$$

The mean velocity $\overline{V}$ in the three equations was determined from $\overline{V} = Q/A$, Q being the measured discharge. The diameter D in all these computations was taken as the measured inside diameter of the pipe as given in Fig. 1, and the pipe was assumed circular. Kinematic viscosity ν was obtained from the measured water temperature using standard tables.

Typical hydraulic grade lines recorded on the manometer board for the three sizes of pipes are shown in Figs. 7 through 9. The slope S was determined from these grade lines or, for low discharges, from grade lines plotted with an expanded vertical scale to obtain more accuracy. For the 24 in. and 18 in. pipes the flow was apparently not fully developed at the upstream taps, as indicated by the upward curve of the grade lines. In these tests the straight downstream section of the grade lines in the last 40 or 50 ft of pipe were used to determine the slope. The grade lines for the 12 in. pipe are straight through all the tap locations.

There are occasional variations from the straight-line portions of the grade lines in Figs. 7 through 9. For example, prominent deviations occur at 72.5 ft and 82.5 ft along the 18 in. pipe. After some investigation it was concluded that these systematic deviations were caused by the pressure taps being located too close, on the downstream side, to one of the spiral joints which occurs during pipe manufacture. Such points were ignored in drawing the grade lines.

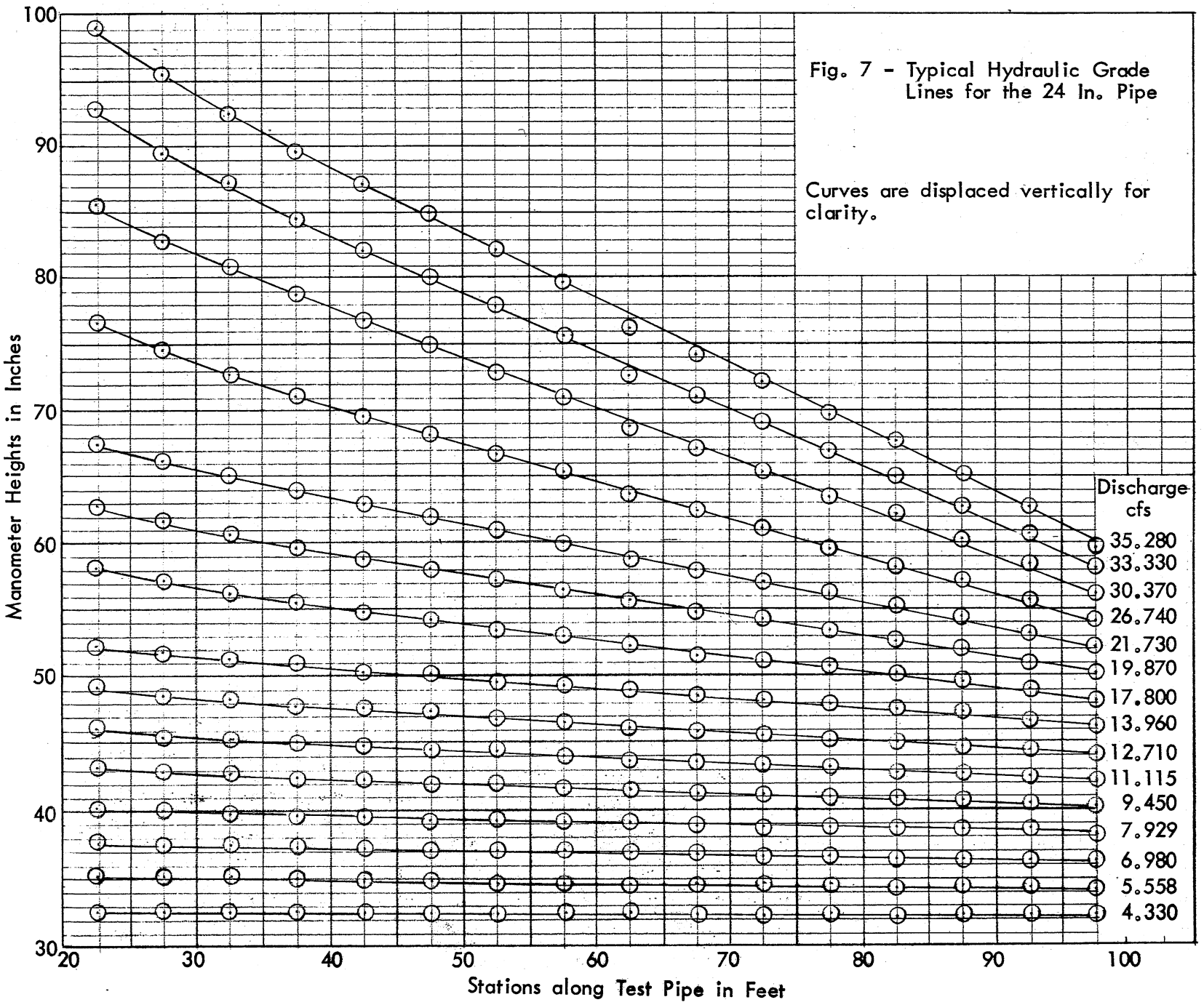

Fig. 7 - Typical Hydraulic Grade Lines for the 24 In. Pipe

Curves are displaced vertically for clarity.

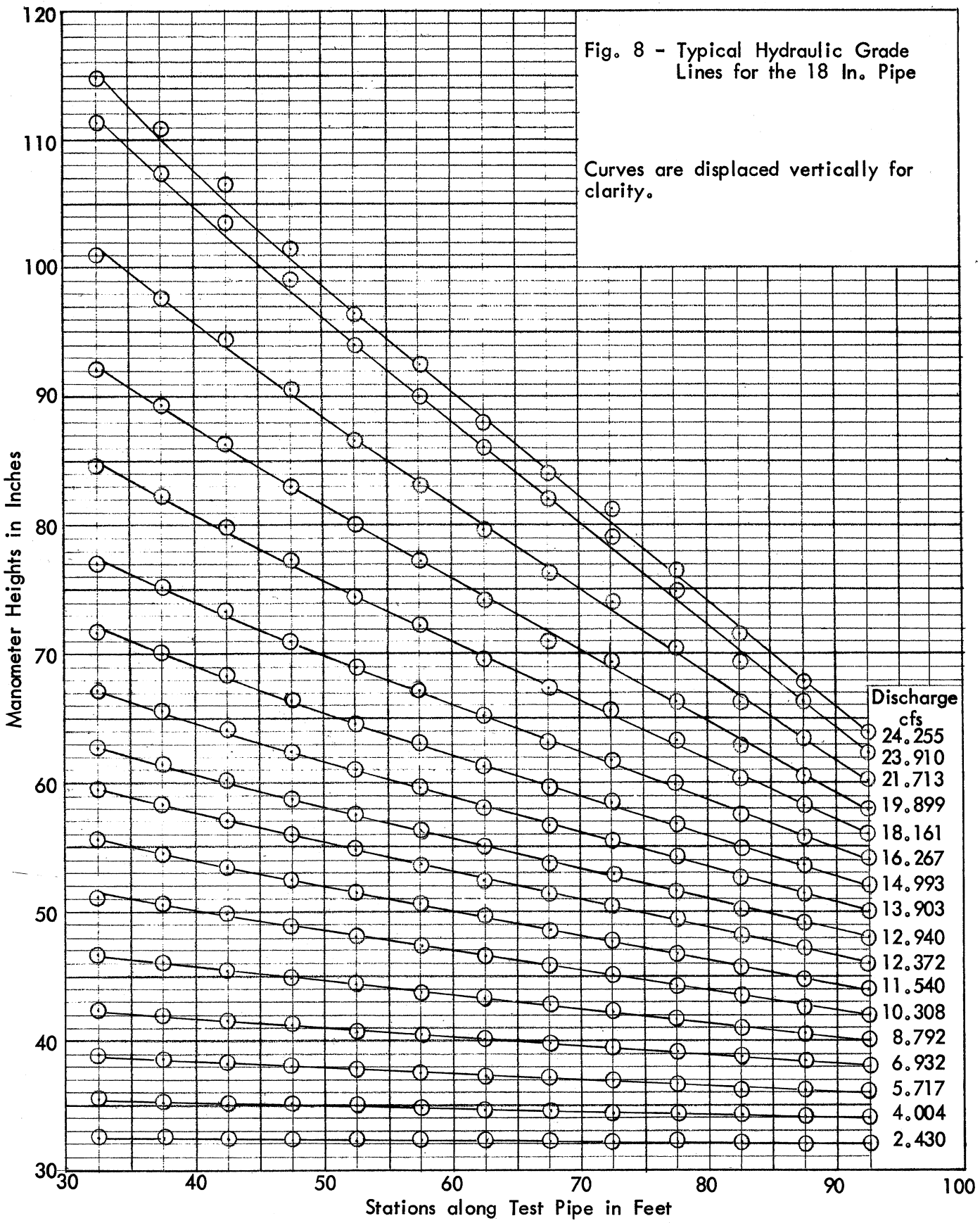
Fig. 8 - Typical Hydraulic Grade Lines for the 18 In. Pipe
Curves are displaced vertically for clarity.
Manometer Heights in Inches
Stations along Test Pipe in Feet
120
110
100
90
80
70
60
50
40
30
30
40
50
60
70
80
90
100
Discharge cfs
24.255
23.910
21.713
19.899
18.161
16.267
14.993
13.903
12.940
12.372
11.540
10.308
8.792
6.932
5.717
4.004
2.430

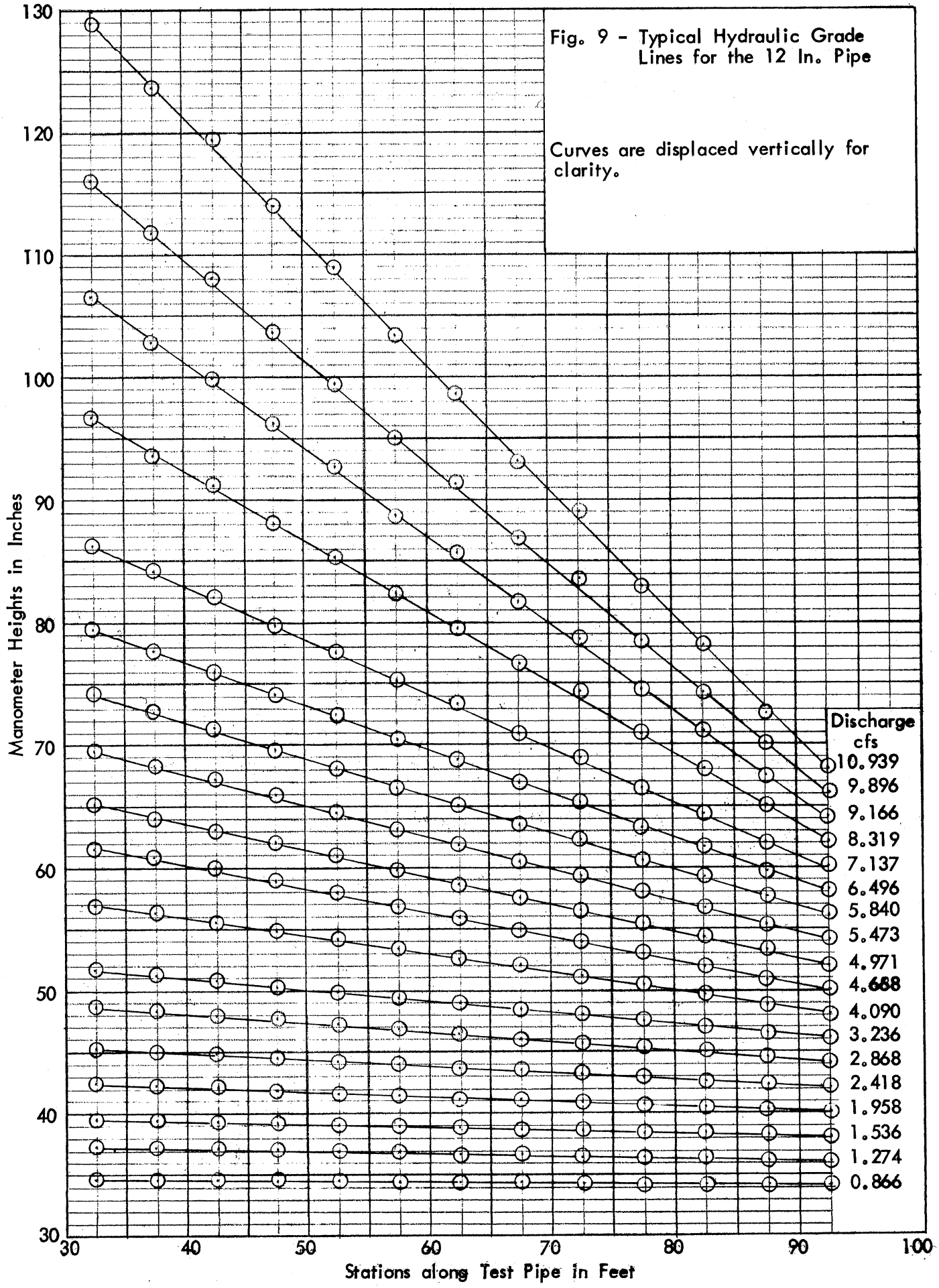
Fig. 9 - Typical Hydraulic Grade Lines for the 12 In. Pipe
Curves are displaced vertically for clarity.
Manometer Heights in Inches
Stations along Test Pipe in Feet
130
120
110
100
90
80
70
60
50
40
30
30
40
50
60
70
80
90
100
Discharge cfs
10.939
9.896
9.166
8.319
7.137
6.496
5.840
5.473
4.971
4.688
4.090
3.236
2.868
2.418
1.958
1.536
1.274
0.866

The variation of the Darcy friction factor f with Reynolds number is shown in Fig. 10 and the variation of the Manning roughness coefficient n with Reynolds number in Fig. 11. Summaries of friction measurements for the three pipes may be found in Tables I through III.

TABLE I. SUMMARY OF FRICTION MEASUREMENTS FOR 24-INCH PIPE

Average measured diameter = 1.998 ft

Q cfs	$\overline{V}$ fps	S per cent	Water Temp. Deg. F	ν ft^2/sec x 10^5	Re x 10^{-6}	Darcy f	Manning n
38.000*	12.121	4.6380	47.2	1.481	1.6352	0.0406	0.0166
35.280	11.254	4.0700	58.5	1.246	1.8046	0.0413	0.0168
33.330	10.632	3.6250	58.5	1.246	1.7049	0.0412	0.0168
30.370	9.687	2.9580	58.5	1.246	1.5533	0.0405	0.0166
26.740	8.530	2.3200	58.5	1.246	1.3678	0.0410	0.0167
21.730	6.931	1.5420	58.5	1.246	1.1114	0.0413	0.0168
19.870	6.338	1.2430	58.5	1.246	1.0163	0.0398	0.0164
17.800	5.678	0.9867	58.5	1.246	0.9105	0.0393	0.0164
13.960	4.453	0.6367	58.5	1.246	0.7141	0.0413	0.0168
12.713	4.055	0.5250	48.0	1.461	0.5545	0.0411	0.0167
12.492	3.985	0.5250	48.0	1.461	0.5450	0.0425	0.0170
11.115	3.545	0.3750	48.0	1.461	0.4848	0.0384	0.0162
9.500	3.030	0.2783	55.5	1.304	0.4642	0.0390	0.0163
9.450	3.014	0.2900	58.5	1.246	0.4833	0.0410	0.0167
7.929	2.529	0.1940	48.0	1.461	0.3459	0.0390	0.0163
6.980	2.226	0.1667	55.5	1.304	0.3411	0.0433	0.0172
5.558	1.773	0.1007	48.0	1.461	0.2425	0.0412	0.0167
4.330	1.381	0.0763	55.5	1.304	0.2116	0.0514	0.0187
1.980	0.632	0.0223	55.5	1.304	0.0968	0.0719	0.0221

*Downstream valve removed

TABLE II. SUMMARY OF FRICTION MEASUREMENTS FOR 18-INCH PIPE

Average measured diameter = 1.508 ft

Q cfs	$\bar{V}$ fps	S per cent	Water Temp. Deg. F	ν ft^2/sec x 10^5	Re x 10^{-6}	Darcy f	Manning n
25.024*	14.011	7.5347	41.5	1.626	1.2994	0.0372	0.0152
24.255	13.581	6.7917	43.5	1.575	1.3003	0.0357	0.0149
23.910	13.387	6.6112	43.5	1.575	1.2818	0.0358	0.0149
21.713	12.157	5.5000	43.5	1.575	1.1640	0.0361	0.0150
20.829*	11.662	5.2222	41.5	1.626	1.0816	0.0373	0.0152
19.899	11.142	4.5555	43.5	1.575	1.0668	0.0356	0.0149
18.297	10.245	3.9028	43.5	1.575	0.9809	0.0361	0.0150
18.161	10.169	3.8333	43.5	1.575	0.9736	0.0360	0.0149
16.267	9.108	3.1112	43.5	1.575	0.8720	0.0364	0.0150
16.052	8.988	3.1667	41.5	1.626	0.8335	0.0380	0.0154
14.993	8.395	2.6112	43.5	1.575	0.8038	0.0360	0.0149
13.903	7.784	2.2500	43.5	1.575	0.7453	0.0360	0.0149
13.557	7.591	2.1528	43.5	1.575	0.7268	0.0363	0.0150
12.940	7.245	1.9792	43.5	1.575	0.6937	0.0366	0.0151
12.372	6.927	1.8055	43.5	1.575	0.6632	0.0365	0.0150
12.015	6.727	1.6597	43.5	1.575	0.6441	0.0356	0.0149
11.644*	6.520	1.6943	41.5	1.626	0.6046	0.0387	0.0155
11.540	6.461	1.5972	43.5	1.575	0.6186	0.0371	0.0152
10.308	5.772	1.2458	43.0	1.588	0.5481	0.0363	0.0150
8.792	4.923	0.9000	43.0	1.588	0.4675	0.0360	0.0149
6.932	3.881	0.5958	43.0	1.588	0.3686	0.0384	0.0154
5.717	3.201	0.4042	43.0	1.588	0.3040	0.0383	0.0154
4.004	2.242	0.1917	43.0	1.588	0.2129	0.0370	0.0151
2.430	1.361	0.0833	43.0	1.588	0.1292	0.0437	0.0165
1.535	0.860	0.0347	43.0	1.588	0.0816	0.0455	0.0168

*Downstream valve removed

TABLE III. SUMMARY OF FRICTION MEASUREMENTS FOR 12-INCH PIPE

Average measured diameter = 0.993 ft

Q cfs	$\bar{V}$ fps	S per cent	Water Temp. Deg. F	ν ft^2/sec x 10^5	Re x 10^{-6}	Darcy f	Manning n
11.540*	14.910	9.5833	44.0	1.562	0.9476	0.0275	0.0122
10.939	14.133	8.4722	42.0	1.613	0.8698	0.0271	0.0121
10.851	14.019	8.3333	42.0	1.613	0.8628	0.0271	0.0121
10.460*	13.514	7.8617	44.0	1.562	0.8589	0.0275	0.0122
9.896	12.786	6.9167	42.0	1.613	0.7869	0.0270	0.0121
9.166	11.842	5.9583	46.0	1.512	0.7775	0.0271	0.0121
8.810*	11.382	5.5555	44.0	1.562	0.7234	0.0274	0.0122
8.319	10.748	4.8055	42.0	1.613	0.6615	0.0266	0.0120
7.137	9.221	3.6767	46.0	1.512	0.6054	0.0276	0.0122
6.496	8.393	2.9653	42.0	1.613	0.5165	0.0269	0.0120
5.840	7.545	2.5000	46.0	1.512	0.4954	0.0281	0.0123
5.473	7.071	2.1875	42.0	1.613	0.4352	0.0279	0.0123
4.971	6.422	1.8055	42.5	1.600	0.3985	0.0280	0.0123
4.668	6.031	1.6250	46.5	1.499	0.3994	0.0285	0.0124
4.090	5.284	1.2388	42.5	1.600	0.3278	0.0283	0.0124
3.236	4.181	0.7750	43.0	1.588	0.2614	0.0283	0.0124
2.886	3.729	0.6417	46.5	1.499	0.2469	0.0295	0.0126
2.418	3.124	0.4513	43.0	1.588	0.1953	0.0295	0.0126
1.958	2.530	0.3247	46.0	1.512	0.1661	0.0324	0.0132
1.536	1.984	0.2000	43.5	1.575	0.1251	0.0324	0.0132
1.274	1.646	0.1463	46.0	1.512	0.1081	0.0345	0.0136
0.866	1.119	0.0833	43.5	1.575	0.0705	0.0425	0.0151
0.699	0.903	0.0625	46.0	1.512	0.0593	0.0489	0.0162
0.394	0.510	0.0278	46.0	1.512	0.0335	0.0684	0.0192

*Downstream valve removed

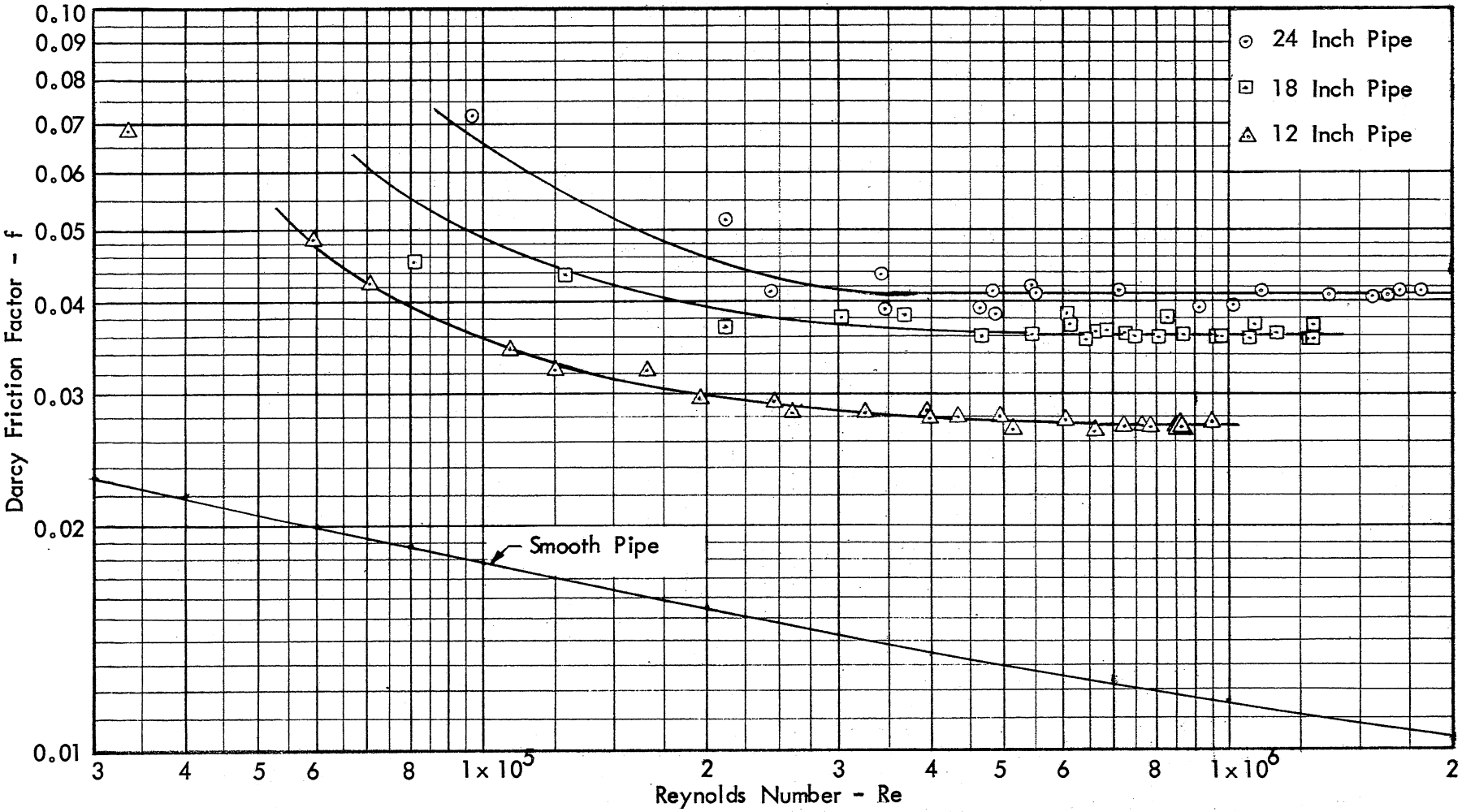

Fig. 10 - Variation of Darcy Friction Factor with Reynolds Number.

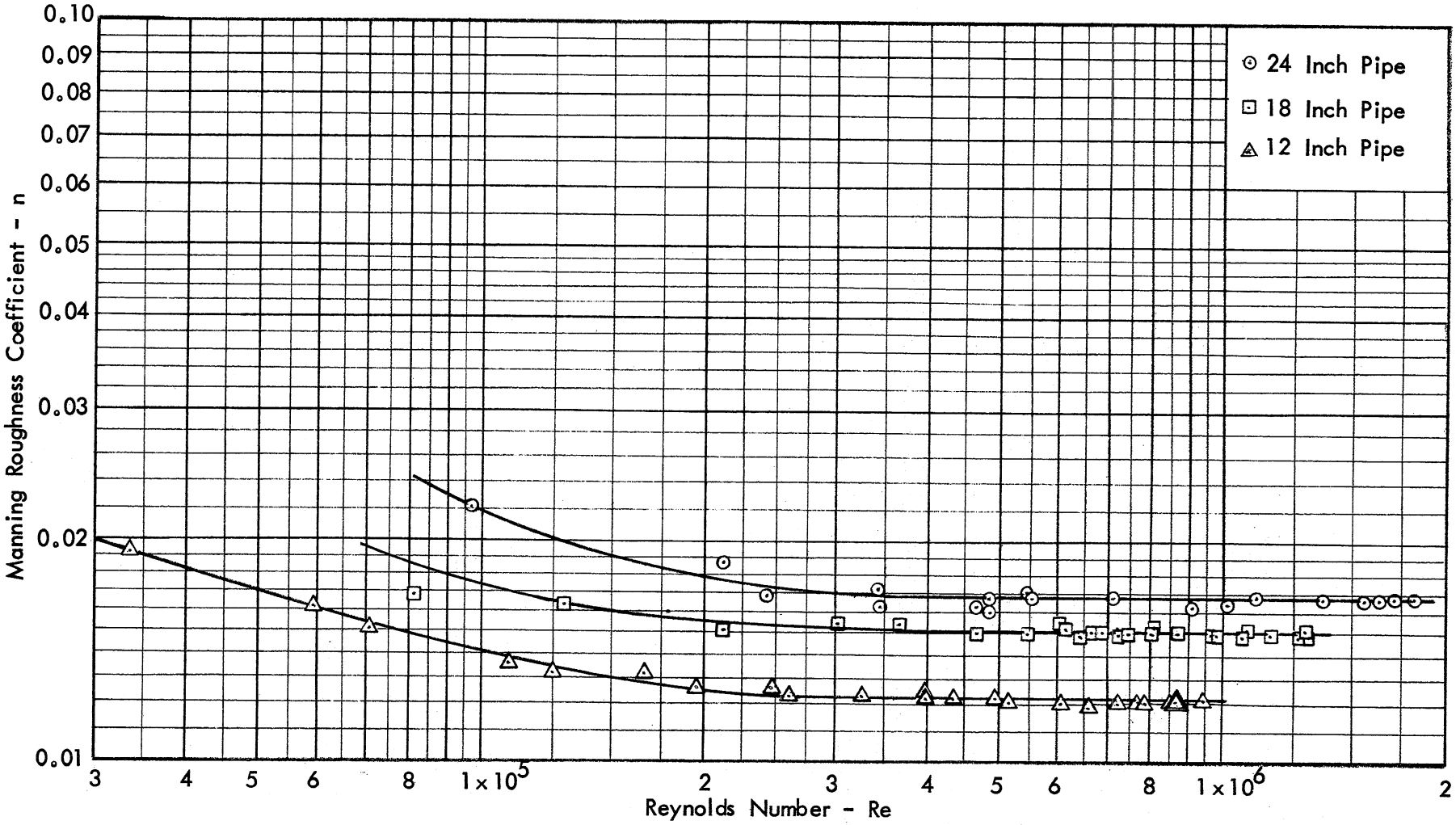

Fig. 11 - Variation of Manning's n with Reynolds Number

IV. VELOCITY PROFILES

A single velocity profile was obtained across a diameter for each size of pipe at a fairly large Reynolds number for that size. Table IV shows discharge and other data for these runs. The velocity data, magnitude and direction, along with the results of some other computations, are given in Tables V through VII.

TABLE IV. RUNS FOR WHICH VELOCITY PROFILES WERE OBTAINED

Pipe Size in.	Q meas. cfs	D ft	$\overline{V}$ fps	$\nu \times 10^5$ ft^2/sec	Re $\times 10^{-6}$	f (Fig. 10)	$V_* = \overline{V}\sqrt{\frac{f}{8}}$ fps	Q Integrated cfs
24	26.54	1.998	8.43	1.304	1.292	0.041	0.604	26.55
18	16.05	1.508	8.96	1.626	0.834	0.037	0.611	16.07
12	9.16	0.993	11.83	1.512	0.777	0.027	0.687	9.24

Velocity magnitudes and directions were obtained using a 3/8 in. diameter Pitot cylinder together with a static tube [2] located as described earlier and shown in Fig. 2. The static tube holes were located nearly opposite the cylinder, and the tube was pointed as nearly as possible in the flow direction by using the direction measured by the Pitot cylinder at the distance the static tube protruded into the pipe (2-1/4 in.). In all three profiles the measured velocity directions at the centers of the pipes apparently varied by 3 or 4 deg from axial. In reducing the data in Tables V through VII, the centerline velocity has arbitrarily been made axial, and the other velocity directions were measured from this reference.

Velocity profiles have been displayed in various ways. Figures 12 through 14 simply show the magnitude plotted across the pipe diameter. Figure 15 shows the magnitude and direction of the velocity in the upper half of the pipe. It may be seen that close to the wall the flow tends markedly toward the helical direction, while the core flow is nearly axial. It may be surmised that within the corrugations the flow is even closer to the helical direction. Figure 16 shows photographs of the helical flow near the walls, marked by dye, emerging from the end of the pipe.

TABLE V. VELOCITY PROFILE DATA FOR 24 IN. PIPE

$\bar{V}$ = 8.43 fps, V_* = 0.604 fps, ν = 1.304 ft^2/sec

Distance from pipe $\mathcal{C}_L$, in.	y, ft (See Fig. 17)	y/R	TOP OF PIPE				BOTTOM OF PIPE			
			V fps	α, deg (See Fig. 15)	U = V cos α fps	$\frac{U_{max} - U}{V_*}$	V fps	α, deg (See Fig. 15)	U = V cos α fps	$\frac{U_{max} - U}{V_*}$
0.0	1.037	1.000	11.87	0.0	11.87	0.00	11.87	0.0	11.87	0.00
2.0	0.870	0.840	11.51	0.0	11.51	0.60	11.55	0.0	11.55	0.53
4.0	0.704	0.679	10.81	1.25	10.81	1.76	10.95	3.75	10.90	1.61
6.0	0.537	0.519	9.93	1.5	9.93	3.22	10.11	5.25	10.02	3.06
7.0	0.454	0.438	9.28	6.25	9.22	4.39	9.79	0.0	9.70	3.59
8.0	0.370	0.357	8.90	7.75	8.82	5.05	9.11	8.25	9.02	4.71
8.5	0.329	0.318	8.53	8.75	8.45	5.66	8.71	11.25	8.54	5.51
9.0	0.287	0.277	8.17	10.75	8.01	6.40	8.43	13.25	8.20	6.07
9.5	0.245	0.236	7.94	9.75	7.77	6.80	8.10	13.75	7.85	6.66
9.75	0.2245	0.217	7.52	12.75	7.34	7.50	7.97	13.75	7.74	6.84
10.0	0.204	0.197	7.41	11.75	7.26	7.64	7.69	16.5	7.30	7.56
10.5	0.162	0.156	7.04	21.25	6.54	8.83	7.41	19.75	6.97	8.11
11.0	0.120	0.116	6.76	23.25	6.21	9.37	7.07	21.0	6.59	8.74
11.25	0.0995	0.096	6.48	26.25	5.81	10.03	6.96	22.5	6.42	9.03
11.5	0.079	0.076	6.14	27.75	5.41	10.70	6.64	27.0	5.84	9.98
11.75	0.058	0.056	5.96	28.50	5.25	10.97	6.36	30.0	5.51	10.53
	0.0	0.0								

TABLE VI. VELOCITY PROFILE DATA FOR 18 IN. PIPE

$\bar{V}$ = 8.96 fps, V_* = 0.611 fps, ν = 1.626 ft^2/sec

Distance from pipe $\mathcal{C}_L$, in.	y, ft (See Fig. 17)	y/R	TOP OF PIPE				BOTTOM OF PIPE			
			V fps	α, deg (See Fig. 15)	U = V cos α fps	$\frac{U_{max} - U}{V_*}$	V fps	α, deg (See Fig. 15)	U = V cos α fps	$\frac{U_{max} - U}{V_*}$
0.0	0.791	1.000	12.58	0.0	12.58	0.00	12.58	0.0	12.58	0.0
1.0	0.704	0.889	12.48	1.5	12.47	0.18	12.45	0.0	12.45	0.21
2.0	0.620	0.784	12.17	2.5	12.08	0.82	12.13	0.0	12.13	0.74
3.0	0.537	0.679	11.73	1.0	11.73	1.39	11.71	1.0	11.71	1.42
4.0	0.454	0.574	11.16	2.0	11.13	2.38	11.11	5.5	11.0	2.58
5.0	0.370	0.468	10.35	4.0	10.23	3.84	10.36	6.0	10.22	3.86
6.0	0.287	0.363	9.60	8.0	9.50	5.04	9.54	9.5	9.40	5.20
6.5	0.245	0.310	9.18	10.0	9.03	5.81	9.18	10.5	9.01	5.84
6.75	0.225	0.285	8.95	11.5	8.80	6.19	8.87	12.0	8.68	6.39
7.00	0.204	0.258	8.66	14.0	8.40	6.84	8.71	14.0	8.47	6.74
7.5	0.162	0.205	8.35	18.0	7.93	7.60	8.17	16.5	7.83	7.78
8.0	0.120	0.152	7.85	22.0	7.28	8.67	7.74	22.0	7.19	8.80
8.25	0.0995	0.126	7.57	25.5	6.82	9.44	7.50	25.5	6.78	9.50
8.5	0.079	0.100	7.33	28.0	6.49	9.95	7.25	29.5	6.31	10.27
8.75	0.058	0.073	6.95	30.5	5.99	10.78	6.90	26.0	6.20	10.42
	0.0	0.0								

TABLE VII. VELOCITY PROFILE DATA FOR 12 IN. PIPE

$\bar{V}$ = 11.83 fps, V_* = 0.687 fps, ν = 1.512 ft^2/sec

Distance from pipe C_L, in.	y, ft (See Fig. 17)	y/R	TOP OF PIPE				BOTTOM OF PIPE			
			V fps	α, deg (See Fig. 15)	U = V cos α fps	$\frac{U_{max} - U}{V_*}$	V fps	α, deg (See Fig. 15)	U = V cos α fps	$\frac{U_{max} - U}{V_*}$
0.0	0.534	1.000	15.61	0.0	15.61	0.00	15.61	0.0	15.61	0.00
0.5	0.492	0.924	15.53	0.0	15.53	0.12	15.46	0.0	15.46	0.22
1.0	0.451	0.846	15.36	0.0	15.36	0.36	15.27	0.0	15.27	0.50
1.5	0.409	0.766	15.04	0.5	15.04	0.83	14.86	2.0	14.84	1.09
2.0	0.367	0.689	14.72	0.5	14.72	1.30	14.49	0.0	14.49	1.63
2.5	0.326	0.611	14.18	1.0	14.18	2.08	13.99	2.0	13.97	2.38
3.0	0.284	0.533	13.58	2.0	13.56	2.98	13.30	5.0	13.20	3.51
3.5	0.242	0.454	13.10	4.5	13.02	3.77	12.68	8.0	12.56	4.4
3.75	0.222	0.416	12.54	7.5	12.40	4.66	12.42	10.0	12.22	4.94
4.0	0.201	0.377	12.29	8.5	12.20	4.96	12.14	12.5	11.86	5.50
4.25	0.180	0.338	11.98	11.0	11.75	5.61	11.69	12.5	11.40	6.14
4.5	0.159	0.298	11.65	14.5	11.30	6.29	11.46	13.0	11.20	6.42
4.75	0.138	0.258	11.18	18.5	10.60	7.30	11.11	15.0	10.73	7.10
5.00	0.117	0.219	11.11	21.5	10.37	7.64	10.81	19.5	10.20	7.89
5.25	0.096	0.180	10.86	22.5	10.05	8.10	10.53	24.5	9.57	8.80
5.5	0.076	0.142	10.63	27.0	9.47	8.94	10.27	25.5	9.30	9.20
5.625	0.065	0.122	10.46	29.5	9.11	9.46	10.15	26.0	9.10	9.49
5.75	0.055	0.103	10.31	30.0	8.92	9.74	10.12	26.0	9.08	9.51
5.875	0.046	0.086	10.07	30.0	8.73	10.0	8.19	25.0	7.40	11.95
	0.0	0.0								

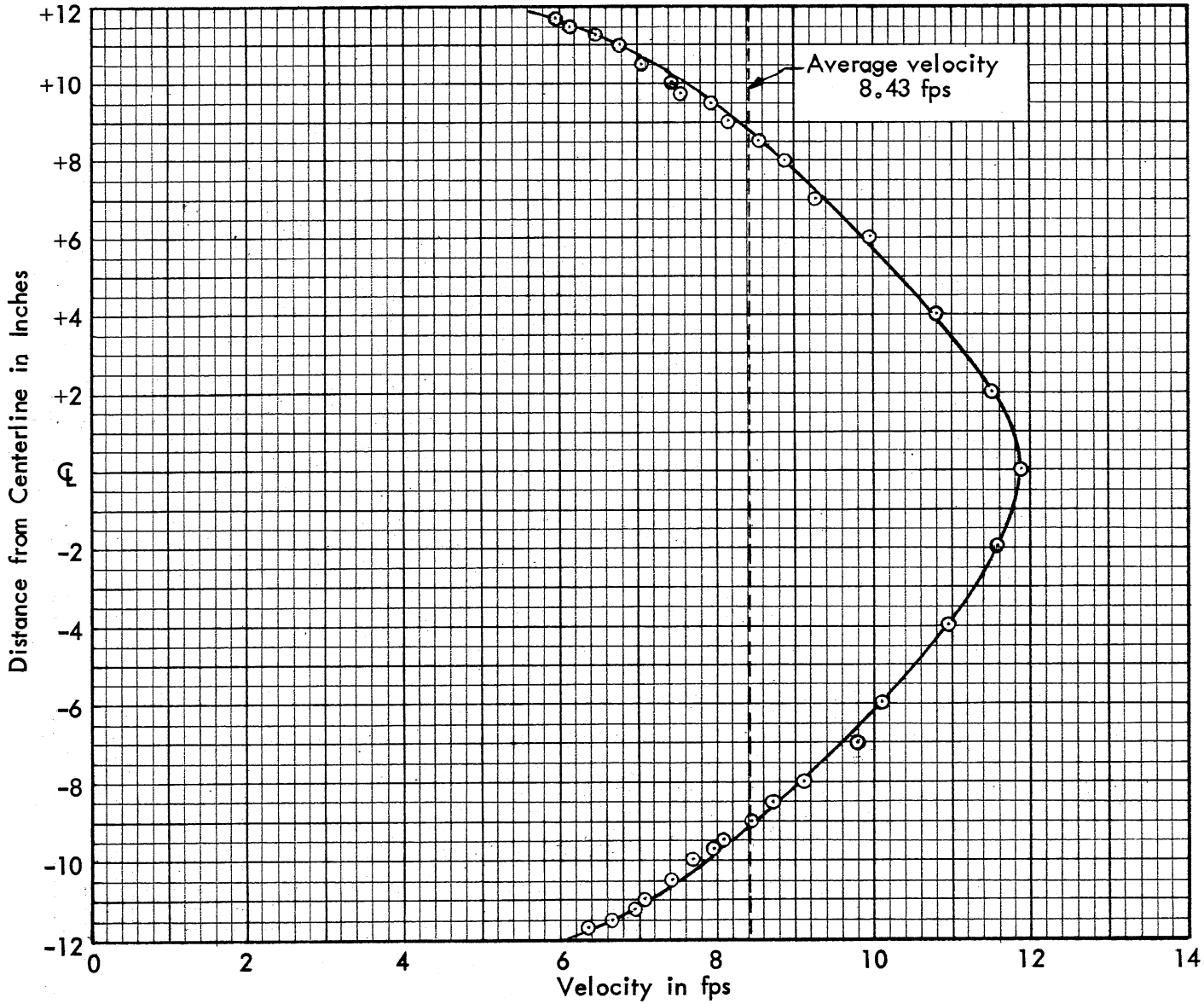

Fig. 12 - Velocity Distribution in 24 In. Pipe

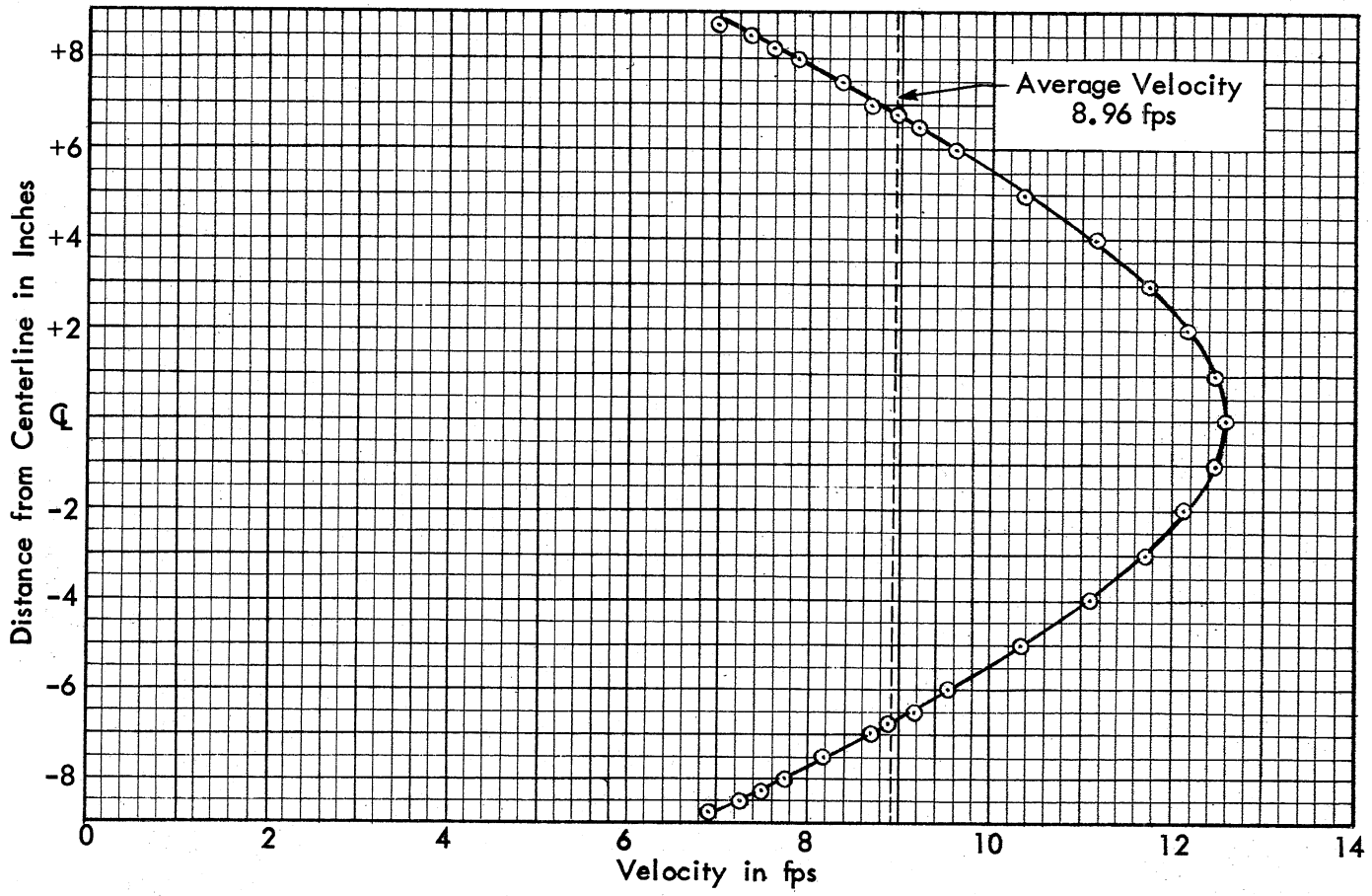

Fig. 13 - Velocity Distribution in 18 In. Pipe

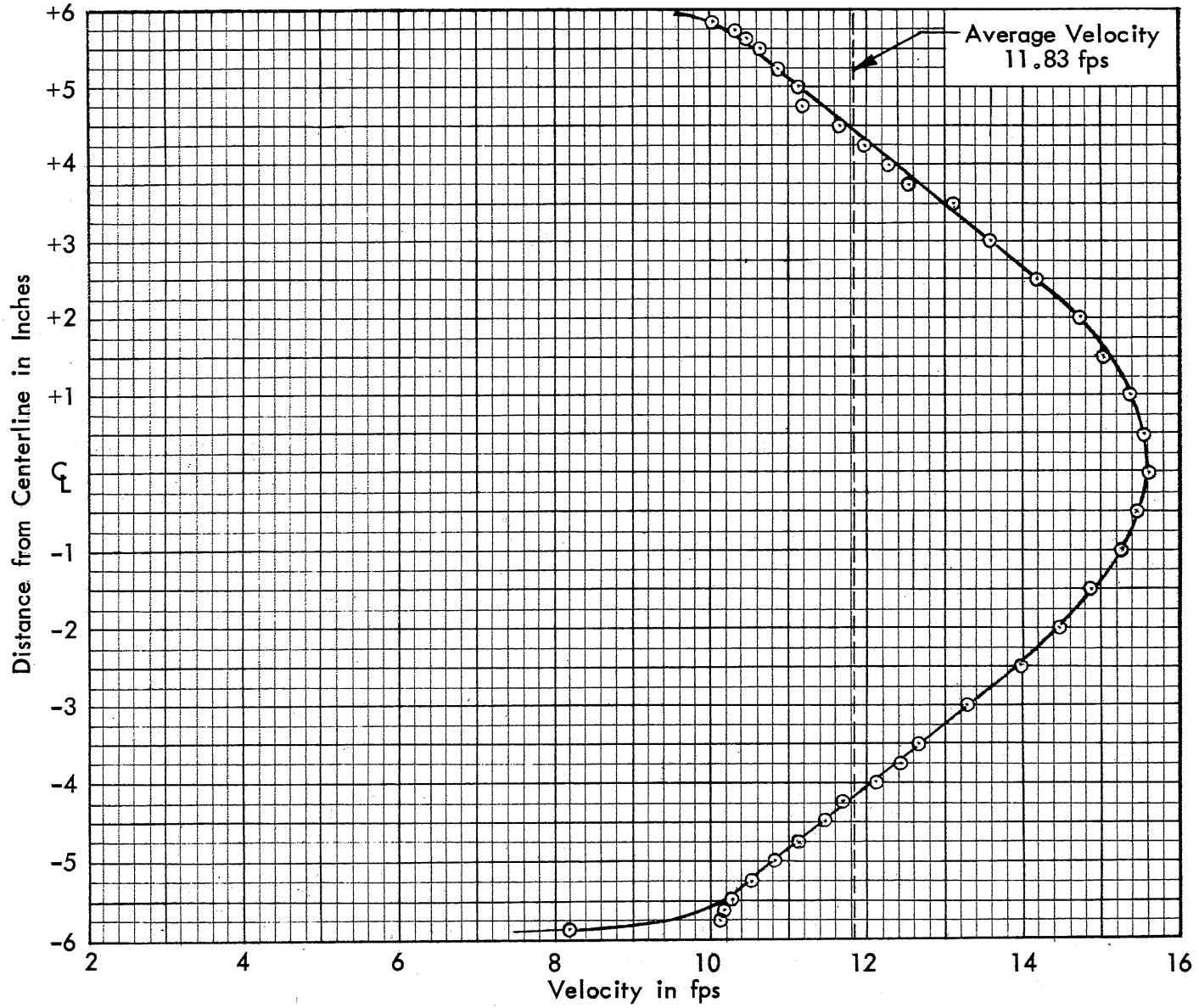

Fig. 14 - Velocity Distribution in 12 In. Pipe

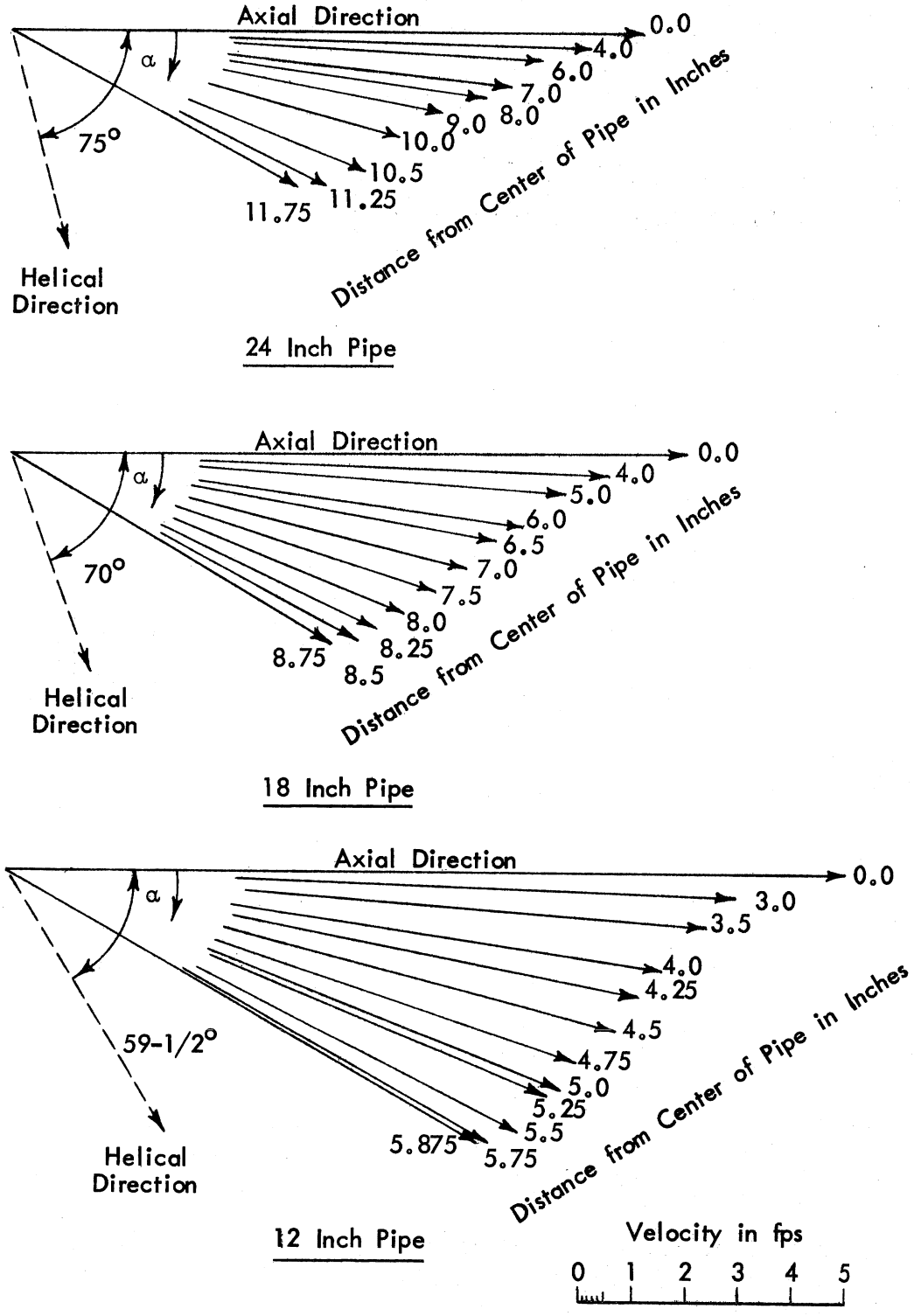

Fig. 15 - Velocity Vectors, Top Halves of Pipes

a. Looking Upstream at the End of the 24 in. Pipe

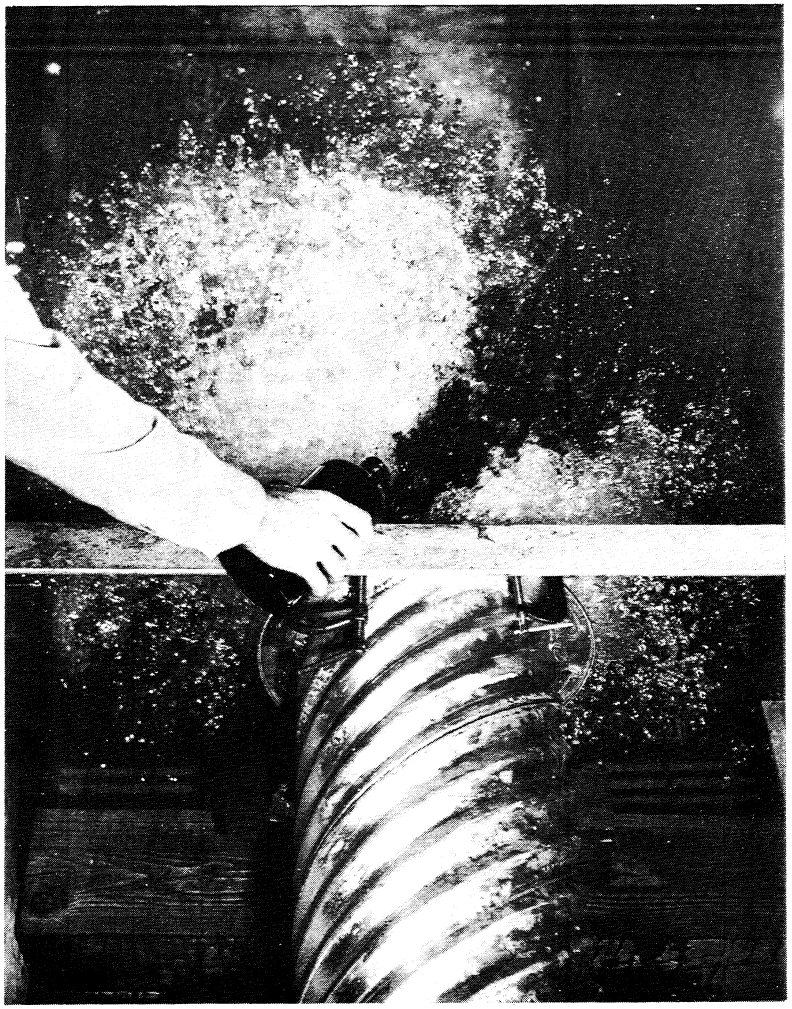

b. Looking Downstream at the End of the 12 in. Pipe

Fig. 16 - Dye Marks the Helical Flow at the Pipe Exit with the Valve Removed

Further analysis was based on the axial component of the velocity. Figure 17 shows the profiles plotted in "defect law" form and Fig. 18 in "law of the wall" form. In these graphs, as shown in the sketch in Fig. 17, the origin of the boundary layer has been taken at the bottoms of the corrugations rather than at the tops as was the case for the analysis of friction factor. Not very many points fall on the straight-line portion of the law-of-the-wall plot, but if the origin had been taken at the tops of the corrugations, even fewer points would have fallen so. Only the upper-half profiles have been plotted for each pipe. Had the lower-half profiles been plotted they would have fallen on the same lines, but with more scatter, as may be seen from Tables V through VII.

On the graph of Fig. 17 two lines have been drawn. One indicates the semi-logarithmic straight-line portion of the data which is seen to extend out from the wall for about 15 per cent of the radius; the other indicates a parabolic law for the remainder of the pipe. The additive constant 4.3 in the semilog law corresponds to the normal value of about 0.8 [3, Fig. 7-29] for an ordinary rough or smooth pipe and to about 2.5 [3, Fig. 7-4] for a zero-pressure-gradient boundary layer. From this viewpoint these pipes act like adverse-pressure-gradient boundary layers. The factor 13.0 in the parabolic law corresponds to 7.2 [3, Fig. 7-49] for a normal pipe. If constant eddy viscosity, ε, is assumed in the central part of the pipe where the parabolic law holds (along with linear shear stress variation across the pipe), the factor 7.2 makes $\varepsilon/RV_* \approx 0.065$, whereas the factor 13.0 makes $\varepsilon/RV_* \approx 0.039$ for all these helically corrugated pipes. It appears that the kinematic eddy viscosity is effectively less in the core regions of these helical pipes than in other rough pipes.

The subtractive constants in Fig. 18 are to be compared with the value for smooth walls given by Clauser [3, Fig. 7-2] of +4.9. The values of $\Delta U/V_*$ shown in the figure are obtained by subtraction from the smooth-pipe law (which lies far above the top of the graph).

The axial velocity components were integrated to obtain discharge. The integration was carried out graphically by plotting the product of axial velocity (mean of top and bottom) and radius measured from the center of the pipe versus radius. The pipe and velocity distribution were assumed to be axially symmetric. For the purpose of this integration, zero velocity was

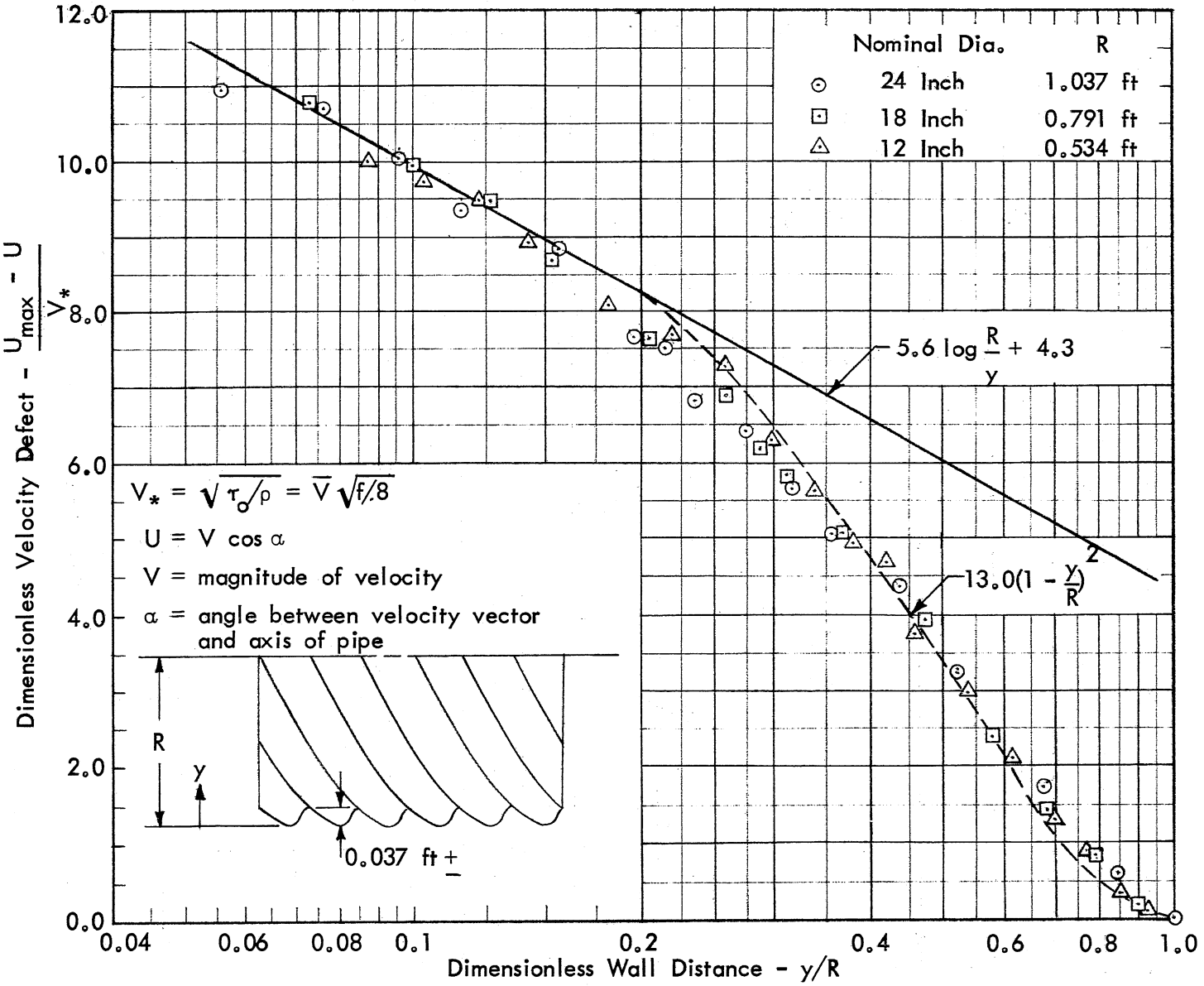

Fig. 17 - Velocity Profiles in Defect-Law Form

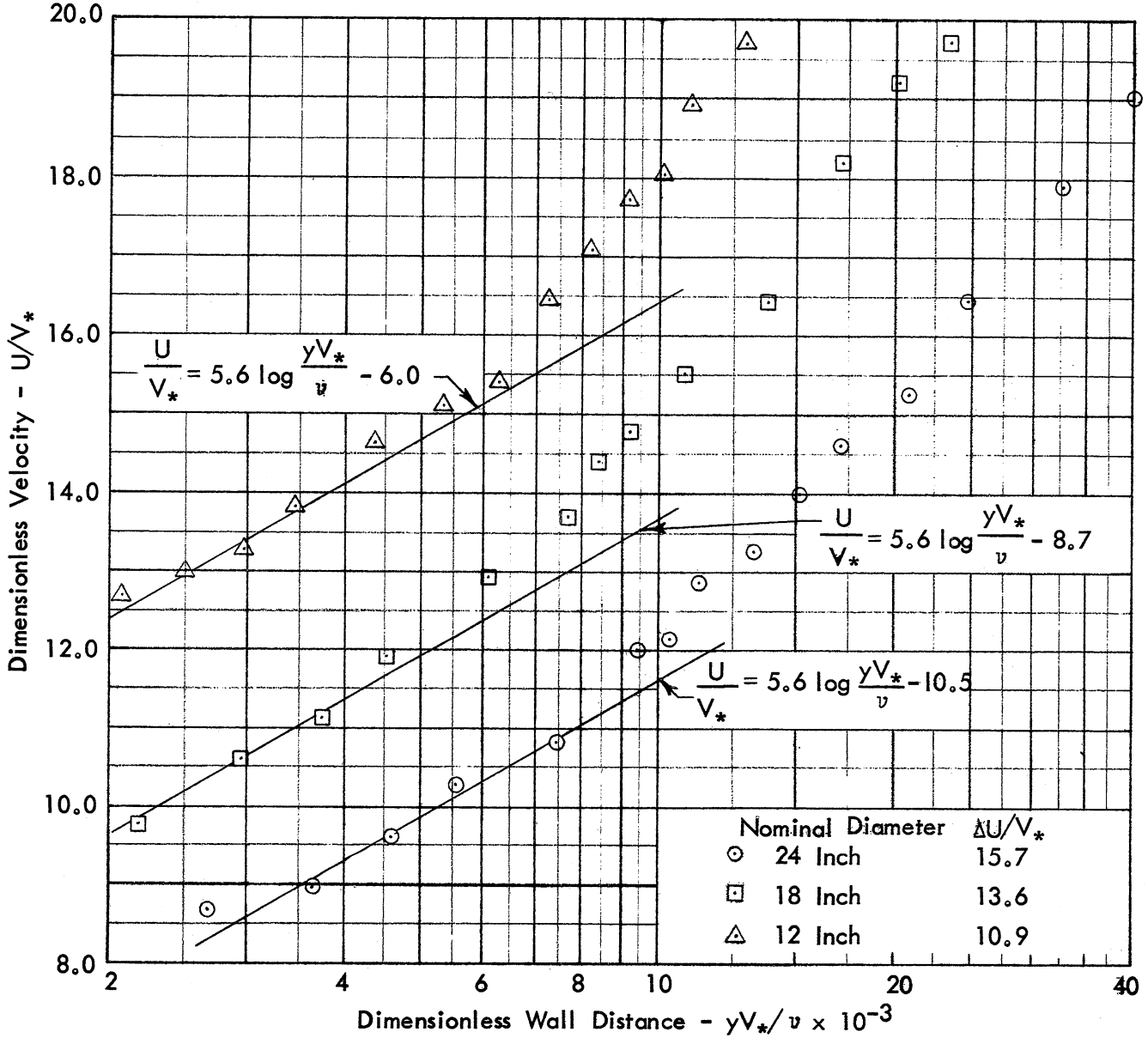

Fig. 18 - Velocity Profiles in Law-of-the-Wall Form

taken in every case as occurring halfway into the corrugations. The integrated discharge for each run is shown in Table IV. The comparisons with measured values are remarkable and lend considerable weight to the measured velocity values. Had zero velocity been taken at the tops of the corrugations (thus neglecting flow through the helixes), the integrated discharge would have been reduced by about 1/30 in each case.

V. POSITION OF HYDRAULIC GRADE LINE AT THE PIPE OUTLET

After completion of the friction and velocity measurements described earlier, the downstream control valve was removed and some additional measurements were made. The procedure described earlier was again used to measure the discharge, water temperature, and hydraulic grade lines with the maximum flow obtainable for all three pipes and with two lower discharges for the 18 in. and 12 in. pipes. The hydraulic grade lines are shown in Figs. 19 through 21 in actual relationship to the pipe.

From these test data the friction factors were computed; they may be found in Tables I through III and on the graphs in Figs. 10 and 11. The values are consistent with those obtained with the valve in place.

The dimension Y, which is the vertical distance from the pipe invert to the hydraulic grade line at the end of the pipe, was also determined. Values of Y/D and $Q/D^{5/2}$ were computed; they are tabulated in Table VIII and plotted in Fig. 22. They are compared there with the results of other investigations as reported by Rice [4]. The data of Blaisdell and Donnelly and of French were the results of tests on smooth lucite pipe. The curve of Straub, Bowers, and Pilch was obtained from tests on 24 in. and 36 in. concrete pipe. The results of investigations by Rice on 8 in. (solid circles and squares) and 12 in. (solid triangles) helical corrugated steel pipe are also plotted. The results of this investigation (plotted as open symbols) agree favorably with the earlier studies at higher values of Y/D and lower discharges, but depart at lower Y/D ratios and higher flows, falling between the smooth lucite pipe and concrete pipe curves and the curve of Rice based on helical corrugated steel pipe.

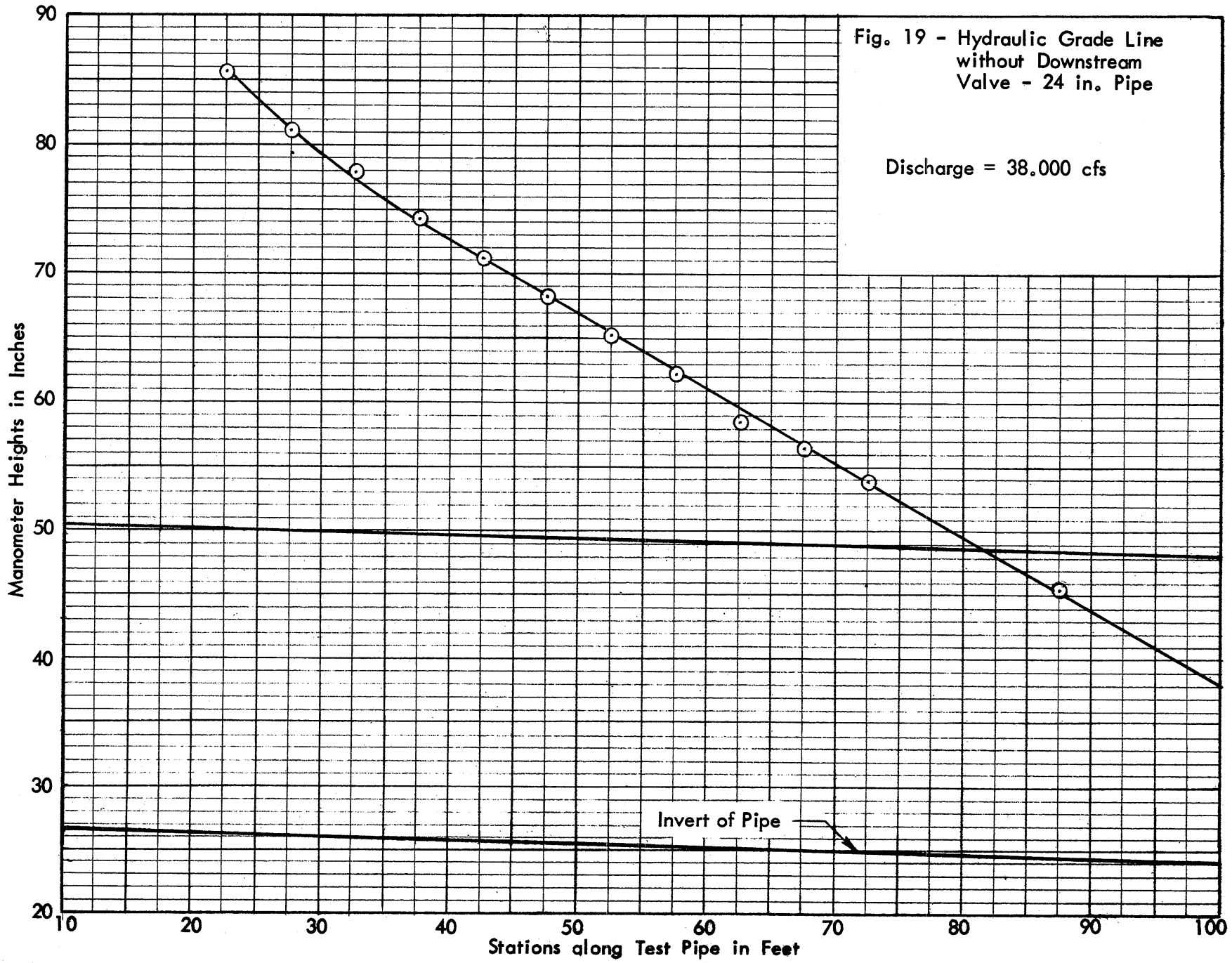
Fig. 19 - Hydraulic Grade Line without Downstream Valve - 24 in. Pipe
Discharge = 38.000 cfs
Manometer Heights in Inches
90
80
70
60
50
40
30
20
Invert of Pipe
10
20
30
40
50
60
70
80
90
100
Stations along Test Pipe in Feet

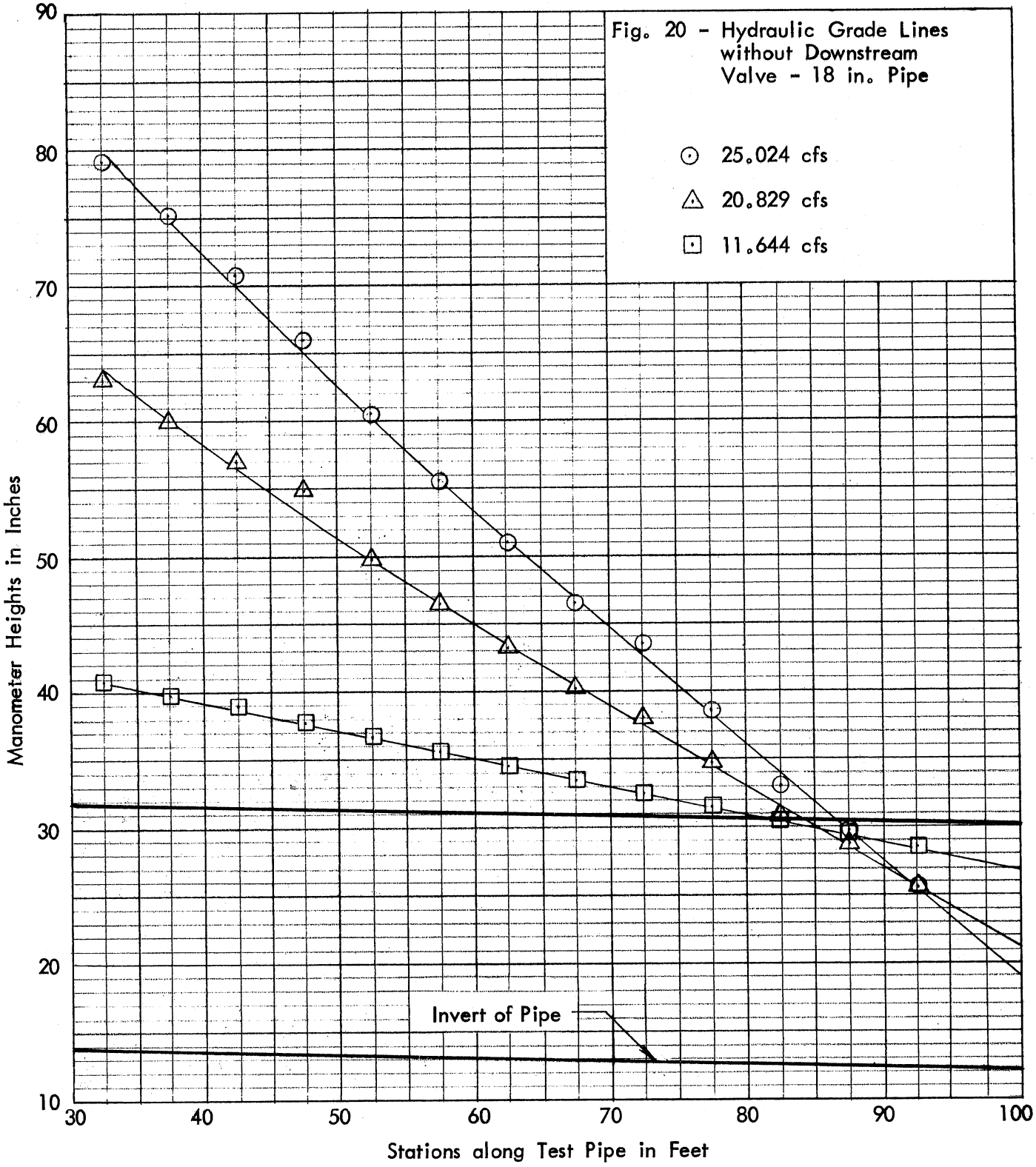
Fig. 20 - Hydraulic Grade Lines without Downstream Valve - 18 in. Pipe
25.024 cfs
20.829 cfs
11.644 cfs
Invert of Pipe
Manometer Heights in Inches
Stations along Test Pipe in Feet
90
80
70
60
50
40
30
20
10
30
40
50
60
70
80
90
100

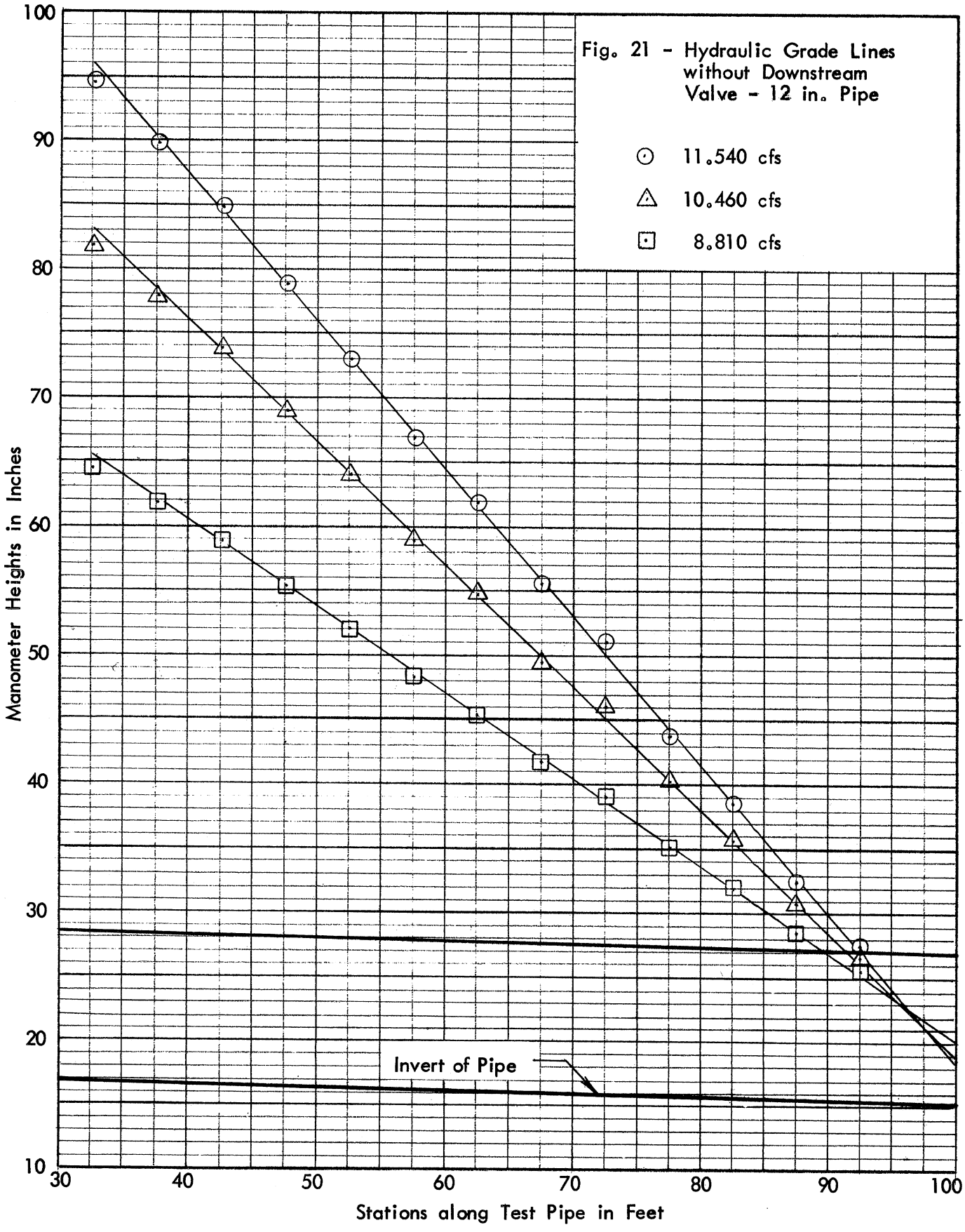
Fig. 21 - Hydraulic Grade Lines without Downstream Valve - 12 in. Pipe
11.540 cfs
10.460 cfs
8.810 cfs
Manometer Heights in Inches
Stations along Test Pipe in Feet
Invert of Pipe
100
90
80
70
60
50
40
30
20
10
30
40
50
60
70
80
90
100

TABLE VIII. POSITION OF HYDRAULIC GRADE LINE AT PIPE OUTLET

Q cfs	D ft	Y ft	Y/D	$Q/D^{5/2}$ $ft^{1/2}/sec$
38.000	1.998	1.191	0.596	6.73
25.024	1.508	0.574	0.381	8.96
20.829	1.508	0.757	0.502	7.46
11.644	1.508	1.222	0.812	4.17
11.540	0.993	0.272	0.274	11.75
10.460	0.993	0.314	0.316	10.65
8.810	0.993	0.414	0.417	8.97

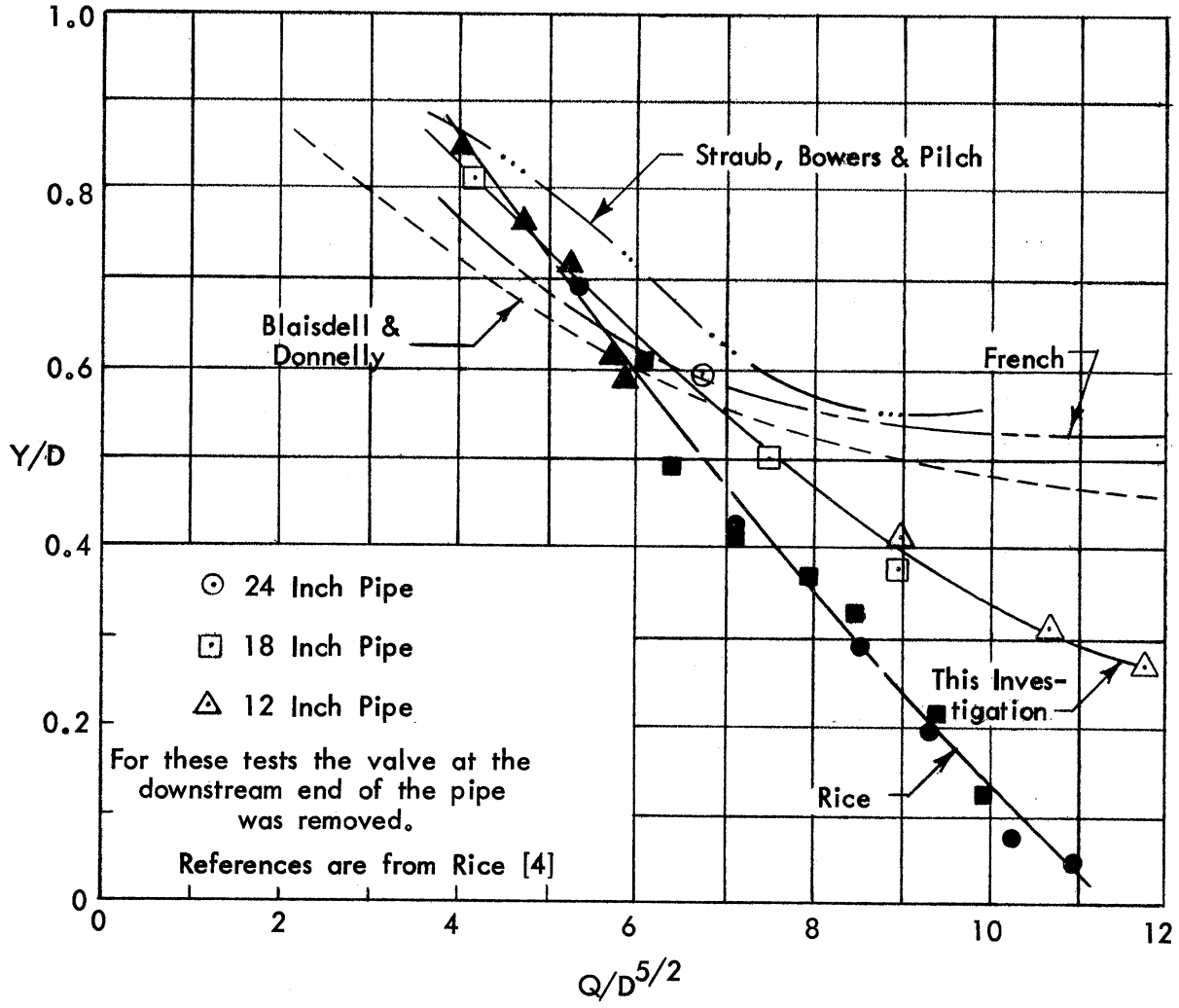

Fig. 22 - Position of Hydraulic Grade Line at the Pipe Outlet

VI. SUMMARY OF FRICTION FACTOR RESULTS

The Darcy friction factor and Manning roughness coefficient values plotted in a reasonably consistent manner, and well defined curves could be drawn through the data points for each pipe size, as shown in Figs. 10 and 11. Some scatter in values is noticeable at lower Reynolds numbers, where the head loss measurements are quite small.

For the 24 in. pipe the curve of Darcy friction factor f is essentially horizontal between Reynolds numbers of 1.8 million down to about 0.5 million with an average f value of 0.041. At lower Reynolds numbers the f values are increasing. For the 18 in. pipe the curve is horizontal from Reynolds numbers of 1.3 million down to about 0.6 million at an average f value of 0.036; below 0.6 million the f values increased. For the 12 in. pipe the average f value is about 0.0272 between Reynolds numbers of 0.95 million down to 0.5 million before increasing in a well defined curve.

The variation of the Manning roughness coefficient n is similar. The n value for the 24 in. pipe is essentially level at about 0.0167 between Reynolds numbers of 1.8 million and 0.4 million before increasing. For the 18 in. pipe the average n value is 0.015 for Reynolds numbers of 1.3 million to 0.4 million. The 12 in. pipe has an average n value of 0.0122 between Reynolds numbers of 0.95 million and 0.3 million before increasing.

It is of some interest to note that at high Reynolds numbers the curve of log f versus helix angle, Fig. 23, is a straight line. This information could be used to interpolate values of f for pipe diameters between 12 in. and 24 in. rolled from the same corrugated sheets as the present pipe, since the helix angle is determined by the diameter. It is even possible to extrapolate f values to diameters larger than 24 in. by this means, but great accuracy should not be claimed for the results. Manning's n does not plot as well as f by this process, but it can always be determined from f by combining Eqs. (1) and (2) to yield

$$n = \frac{0.416}{\sqrt{g}} D^{1/6} f^{1/2} \qquad (4)$$

in English units.

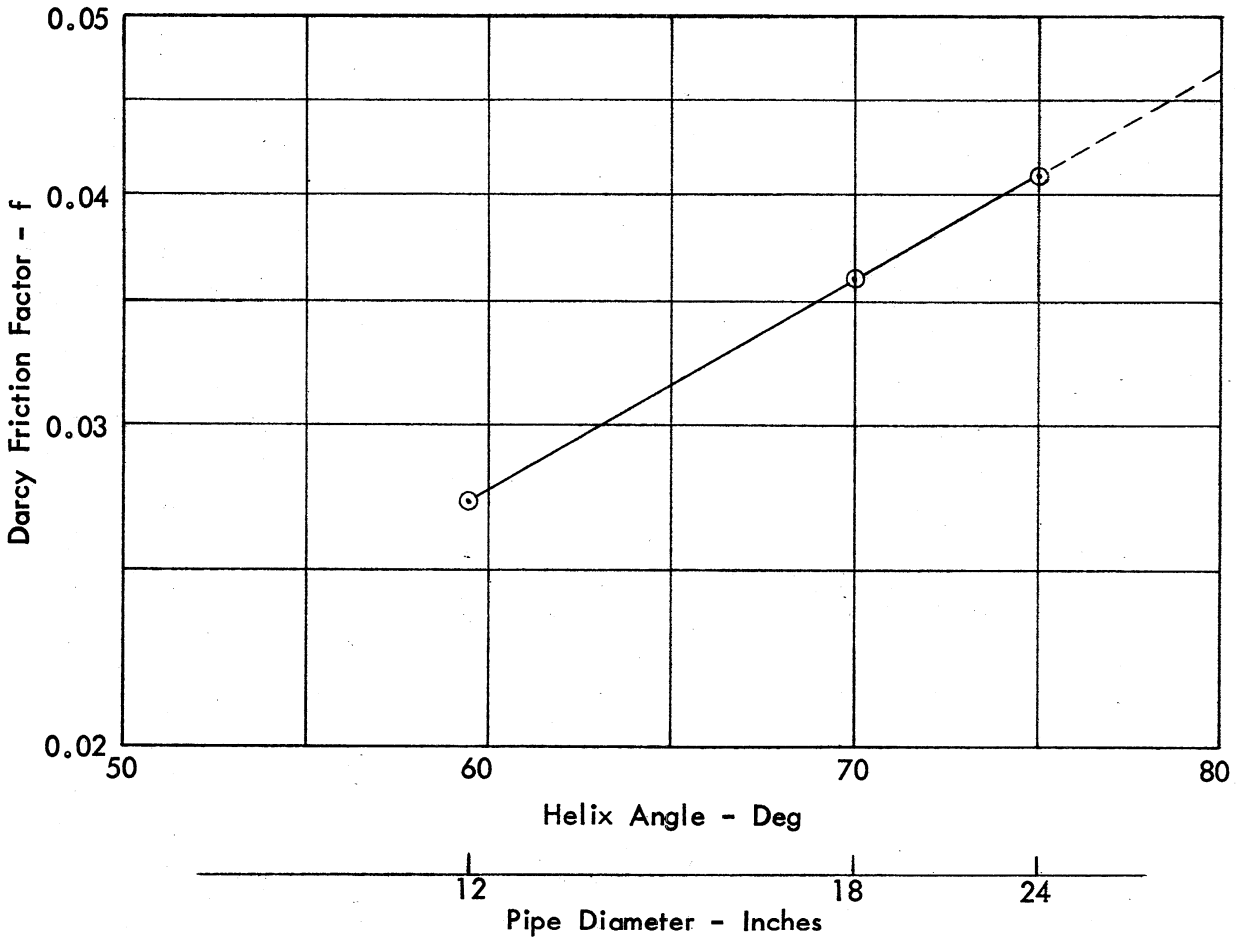

Fig. 23 - Darcy Friction Factor as a function of Helix Angle at High Reynolds Numbers

It should be observed that the friction factor values obtained in this report are for fully developed flow in straight and uniform pipe without joint losses. Great care was exercised to obtain these results. In field work joints are not likely to be so carefully made, the pipe alignment will not be as good, there will be entrance and exit losses, and there may be some leakage through joints and seams. In designing field pipe lines good judgment must be used in calculating these additional factors to determine the total head loss.

LIST OF REFERENCES

[1] Webster, M. J. and Metcalf, L. R., "Friction Factors in Corrugated Metal Pipe," Journal of the Hydraulics Division, Proceedings of the ASCE, Vol. 85, No. HY9, September 1959, pp. 35-67.

[2] Silberman, E., The Pitot Cylinder, Circular No. 2, University of Minnesota, St. Anthony Falls Hydraulic Laboratory, October 1947.

[3] Hinze, J. O., Turbulence, McGraw-Hill, New York, 1959.

[4] Rice, C. E., Friction Factors for Helical Corrugated Pipe, ARS 41-119, Agricultural Research Service, U.S. Department of Agriculture, February 1966.